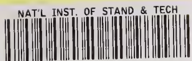
NAT'L INST. OF STAND & TECH
A11106 323464

NIST
PUBLICATIONS

NIST SPECIAL PUBLICATION **260-145**

U. S. DEPARTMENT OF COMMERCE/Technology Administration
National Institute of Standards and Technology

Standard Reference Materials®

Standard Reference Material 2538 for Polarization-Mode Dispersion (Non-Mode-Coupled)

**Paul A. Williams, Shelley M. Etzel,
Jonathan D. Kofler, and Chih-Ming Wang**

NIST
[Nati]onal Institute of Standards and Technology
[Tech]nology Administration, U.S. Department of Commerce

QC
100
.U57
no. 260-145
2002
c. 2

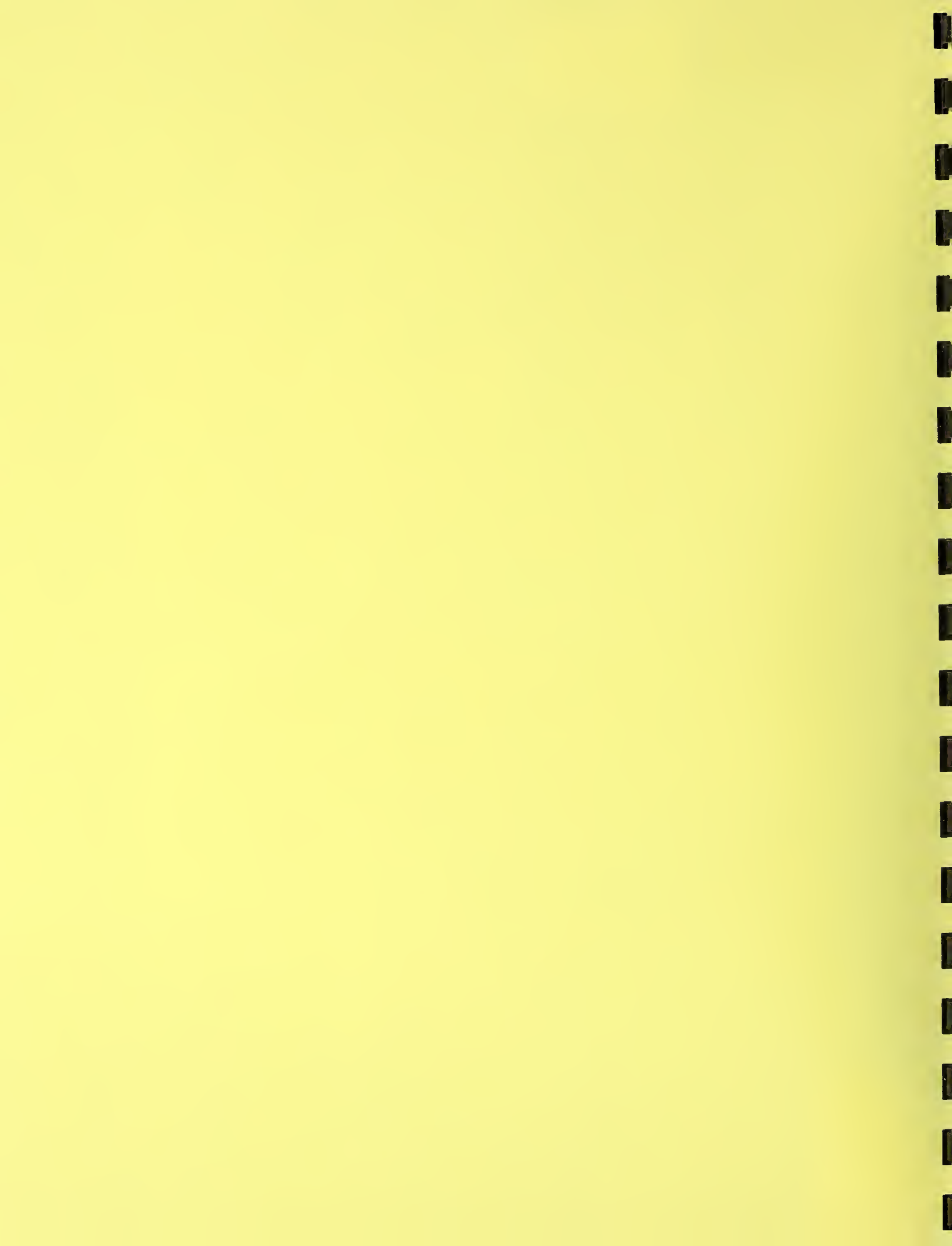

NIST Special Publication 260-145

Standard Reference Materials®

Standard Reference Material 2538 for Polarization-Mode Dispersion (Non-Mode-Coupled)

Paul A. Williams, Shelley M. Etzel, and Jonathan D. Kofler
Optoelectronics Division
Electronics and Electrical Engineering Laboratory
National Institute of Standards and Technology
Boulder, CO 80305-3328

Chih-Ming Wang
Statistical Engineering Division
Information Technology Laboratory
National Institute of Standards and Technology
Boulder, CO 80305-3328

U.S. DEPARTMENT OF COMMERCE, *Donald L. Evans, Secretary*
TECHNOLOGY ADMINISTRATION, *Phillip J. Bond, Under Secretary of Commerce for Technology*
NATIONAL INSTITUTE OF STANDARDS AND TECHNOLOGY, *Arden L. Bement, Jr., Director*

Issued July 2002

Certain commercial equipment, instruments, or materials are identified in this paper in order to specify the experimental procedure adequately. Such identification is not intended to imply recommendation or endorsement by the National Institute of Standards and Technology, nor is it intended to imply that the materials or equipment identified are necessarily the best available for the purpose.

National Institute of Standards and Technology Special Publication 260-145
Natl. Inst. Stand. Technol. Spec. Publ. 260-145, 44 pages (July 2002)
CODEN: NSPUE2

U.S. GOVERNMENT PRINTING OFFICE
WASHINGTON: 2002

For sale by the Superintendent of Documents, U.S. Government Printing Office
Internet: bookstore.gpo.gov — Phone: (202) 512-1800 — Fax: (202) 512-2250
Mail: Stop SSOP, Washington, DC 20402-0001

Standard Reference Material 2538 for Polarization-Mode Dispersion (Non-Mode-Coupled)

Contents

1. Introduction 1

2. Artifact Description 3

3. Certification Value 5

4. Certifying Measurements 6

5. Uncertainty Analysis 8
   5.1 "High-Accuracy" Value 8
   5.2 Wavelength-Extrapolated Range 9

6. References 13

Appendix A: Sample Certificate (SRM 2538) 15

Appendix B: Fixed Analyzer Measurements and Uncertainty 23
   B.1. Fixed Analyzer Measurement Description 23
   B.2. Fixed Analyzer Measurement Uncertainty 24

Appendix C: Description of NIST Jones Matrix Eigenanalysis Polarimeter 31
   ("Rotating-Wave-plate Stokes polarimeter for differential group delay
   measurements of polarization-mode dispersion")

Appendix D: Birefringence of Quartz 41

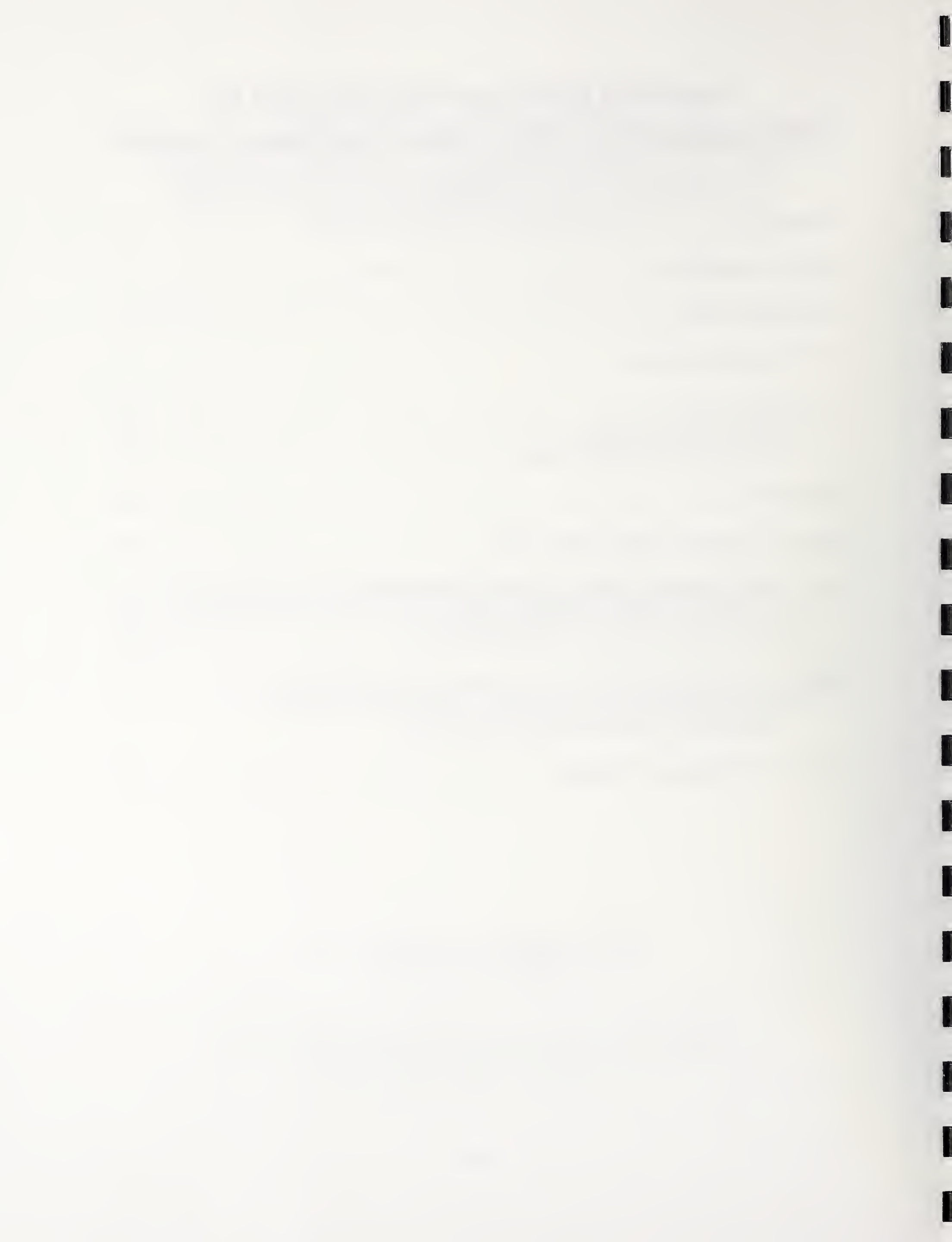

NIST Special Publication 260-145

Standard Reference Material 2538 for Polarization-Mode Dispersion (Non-Mode-Coupled).

Paul A. Williams, Shelley M. Etzel, Jonathan D. Kofler

Optoelectronics Division
Electronics and Electrical Engineering Laboratory
National Institute of Standards and Technology
Boulder, CO 80305

Chih-Ming Wang

Statistical Engineering Division
Information Technology Laboratory
National Institute of Standards and Technology
Boulder, CO 80305

A temperature-controlled, single-mode-fiber-pigtailed quartz plate has been assembled as an artifact standard for polarization-mode dispersion (non-mode-coupled). The design parameters and performance of this device are discussed. The artifact, Standard Reference Material SRM 2538, provides an environmentally stable value of wavelength-averaged differential group delay (DGD) that is nominally 300 fs. This value is certified for any wavelength span of 50 nm or greater that is contained in the 1250-1650 nm window. A slightly higher accuracy number is also provided for wavelength-averaged DGD over the ~1480-1570 nm window. Details of the certifying measurements and associated uncertainties are given.

Keywords: birefringence, DGD, differential group delay, PMD, polarization-mode dispersion, standard reference material, SRM

1. Introduction

In order to provide a stable artifact exhibiting non-mode-coupled polarization-mode dispersion, the National Institute of Standards and Technology (NIST) has tested and certified Standard Reference Material SRM 2538 "Polarization-Mode Dispersion (Non-Mode-Coupled)." This document describes the artifact including its design and performance, and the measurement systems and procedures used to certify the artifact. Uncertainty of the artifact is described in detail based on uncertainties of the measurement techniques.

We begin this document with a few definitions:

Polarization-mode dispersion (PMD)

PMD in an optical element comes about as the result of birefringence yielding different propagation velocities for different polarization states. An element exhibiting PMD has "fast" and "slow" polarization axes, along which the light has its fastest and slowest group velocities.

In the absence of polarization-dependent loss, these axes are orthogonal. In the simplest case of PMD the orientation of these axes is independent of wavelength. This is true when there is no coupling between the polarization modes. This is called the "non-mode-coupled" case. A simple example of non-mode-coupled PMD is a single birefringent crystal. An example of a mode-coupled device is one with several birefringent crystals in series with their optic axes non-parallel. This latter device also has fast and slow polarization axes, but their orientation is a function of wavelength.

Differential Group Delay (DGD)
DGD is the difference in propagation delay between the fast and slow axes, and is the metric used to describe the strength of PMD. (However, "PMD" is sometimes used loosely to mean DGD or average DGD.) In this document, "PMD" will refer to the phenomenon and "DGD" will refer to its magnitude.

Need for PMD Artifact Standard
The problem with PMD in optical telecommunication systems is that it causes pulse broadening, which leads to increased bit error rate. The PMD in fibers generally exhibits polarization mode-coupling, while PMD in individual optical elements is more often non-mode-coupled. This work arose out of the need to verify the performance of PMD measurement equipment and techniques on non-mode-coupled devices. In order to accomplish this, we built a device exhibiting approximately 300 fs of non-mode-coupled DGD and have certified the wavelength averaged DGD to an expanded uncertainty of less than 1.5 %. For calibrations of mode-coupled PMD, NIST already offers a Standard Reference Material (SRM 2518).

Certification of SRM 2538
Certified values of wavelength-averaged (mean) DGD of the artifact are provided to the customer through the Standard Reference Material Certificate (Appendix A). A look-up table provides certified values of mean DGD over any wavelength within the 1250 nm to 1650 nm window, subject to a 50 nm minimum span width requirement. These values have been determined using the measurement technique of Jones Matrix Eigenanalysis (JME) [1] to measure the mean DGD directly over a 1480 nm to 1570 nm range and then extrapolating this value to other wavelength ranges using a knowledge of the group birefringence of quartz (the birefringent material in SRM 2538). These extrapolated values are verified by using the Fixed Analyzer (FA) technique (Appendix B) to measure mean DGD over the nominally 1250 nm to 1650 nm wavelength range. These certified values are reported with an uncertainty based on a worst-case estimate so that one uncertainty value applies to all mean DGD values reported within the 1250 nm 1650 nm window.

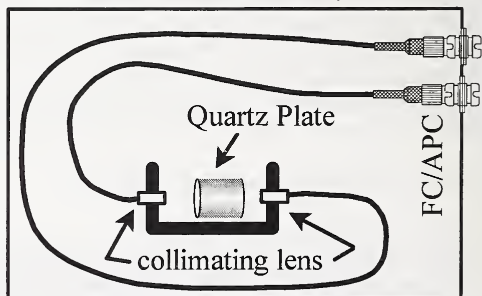

Fig. 1. Schematic diagram of SRM 2538 showing pigtailed quartz plate.

A "high-accuracy" value of mean DGD averaged over the nominal wavelength range of 1480 nm to 1570 nm is also provided. Since this value is measured directly by the JME technique with no

need for wavelength extrapolation, it has the lowest uncertainty.

2. Artifact Description

SRM 2538 (the "artifact") is based on a single quartz plate pigtailed with single-mode fiber. The quartz plate provides the non-mode-coupled PMD and is nominally 1 cm in length, cut with the z-axis parallel to the exit and entrance faces. The fibers are pigtailed to the quartz plate through collimating lenses with an air gap between the lenses and the quartz plate. The total length of the pigtails is less than 2 m, and they are terminated in FC/APC style connectors (2.15 mm wide key). The fiber leads are coiled and fastened inside the box with a bend radius of approximately 3.5 cm. The device is packaged with a thermoelectric cooler to maintain the quartz plate at a temperature of nominally 45 °C. The crystal temperature can be monitored through an external BNC style connector. The voltage on the BNC is proportional to the internal temperature in kelvins with a coefficient of 10 mV/K. The relationship between the Kelvin and Celsius scales is T(K) = T(°C) + 273.15 where T(K) is the temperature in kelvins and T(°C) is the temperature in degrees Celsius. So, a reading of 3.18 V would be 318 K or 45 °C. A diagram of the artifact is shown in Fig. 1.

Table 1. Specifications of SRM 2538 artifact (adherence to these specifications is not certified by NIST).

Parameter	Specified value
Insertion loss	< 3 dB
Internal temperature stability	±5 °C
Return loss	> 50 dB
Storage temperature	15 – 30 °C
Minimum internal fiber bend radius	3.5 cm

The SRM 2538 artifacts are assembled by an external vendor (outside of NIST). Table 1 lists the important target specifications of the artifact. Adherence to these values is not certified by NIST; these specifications are supplied merely to aid in the replication of similar artifacts. However, many of these parameters are important to the stable operation of the device. Details are described below.

Temperature Control

The temperature of the quartz plate is controlled to ±5 °C to reduce error due to the temperature dependence of the birefringence of quartz. To assess the uncertainty induced by a ±5 °C variation, we measured the temperature dependence of a typical SRM 2538 artifact. Assuming linear behavior with temperature, we measured the mean DGD at two different temperatures. With the artifact powered up, the internal temperature was 43.8 °C and the mean DGD over a nominal 1480 nm to 1570 nm range was 313.1 fs. With the power turned off for several hours, the artifact temperature was 21.5 °C and the mean DGD was 314.8 fs. This gives a temperature slope of 0.076 fs/°C. We find this number to be about twice as large as would be expected from the temperature dependence of the retardance of quartz $\gamma = (1/\Delta nL)\mathrm{d}(\Delta nL)/\mathrm{d}T =$ $-0.0001232\ {}^{\circ}\mathrm{C}^{-1}$ [2] (T is temperature, L is physical path length in the quartz, and Δn is the phase birefringence). Of course, γ refers to phase birefringence, and our measurement reports the

temperature dependence of the group birefringence Δn_g. However, we don't expect that the difference between $d\Delta n_g/dT$ and $d\Delta n/dT$ is large enough to cause this discrepancy. Rather, it is likely explained by the presence of stress birefringence in the quartz plate, or fiber effects, etc.

With the empirical temperature dependence of the artifact, we see that variation of the temperature within the qualified range (±5 °C) will not significantly affect the measured mean DGD (compared to the nominal 4 fs expanded uncertainty of the final certification). To ensure proper operation of the device, it should be powered up for 1 hour before measurements are made. Then, after 1 hour, the temperature monitor voltage should be checked to verify that the temperature agrees with the target value (listed in the SRM certificate) to within the range specified in Table 1.

Multiple Reflection Suppression

Multiple reflections within the quartz plate can affect the measured DGD of the device (adding a ripple in wavelength). To minimize this effect, the quartz plate has a single-layer MgF_2 anti-reflection coating (centered at 1425 nm). The intensity reflection coefficient was not measured, but is estimated to be 1 to 2 % over the 1200 nm to 1700 nm spectrum. In an effort to further reduce multiple reflections, later generations of the artifact were assembled with the quartz plate both anti-reflection coated and tilted by an angle of 4 to 5° with respect to the incoming beam. This causes any multiply-reflected light traveling in the forward direction to be deviated sufficiently to miss the output collimating lens (Fig. 2).

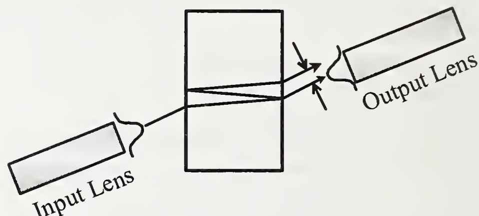

Figure 2 Tilting the waveplate with respect to the collimating lenses causes a forward-reflected beam to miss collection in the output collimating lens.

Return Loss

Return loss is sometimes considered to be a measure of the level of multiple reflections occurring within the device. Unfortunately, this provides a poor estimate for SRM 2538 since return loss measures reflections that go backward toward the source and DGD uncertainty comes from multiple reflections that go forward away from the source. Return loss is kept low (via FC/APC connectors, anti-reflection coatings, and the tilted quartz plate) to prevent light from returning to the source, but a low return loss alone is not a guarantee against forward reflected light.

Storage Temperature

In order to verify the stability of the artifacts with storage temperature, each device was cycled from 0 °C to 50 °C two to four times (1 hour ramp times and 1 hour dwell times at each endpoint). The mean DGD was measured before and after cycling to verify that no significant (outside the certified uncertainty) changes in mean DGD occurred. The difference in mean DGD before and after temperature cycling yielded no statistically significant difference for any of the artifacts. To illustrate the long-term stability, Fig. 3 shows a control chart for one artifact measured over approximately two years with no significant variation in measured mean DGD (in

spite of the temperature cycling indicated in the figure). The recommended storage temperature of the device is 15 °C to 30 °C. However, as demonstrated, the artifact can experience temperatures between 0 °C and 50 °C for short periods of time without harm to the certification.

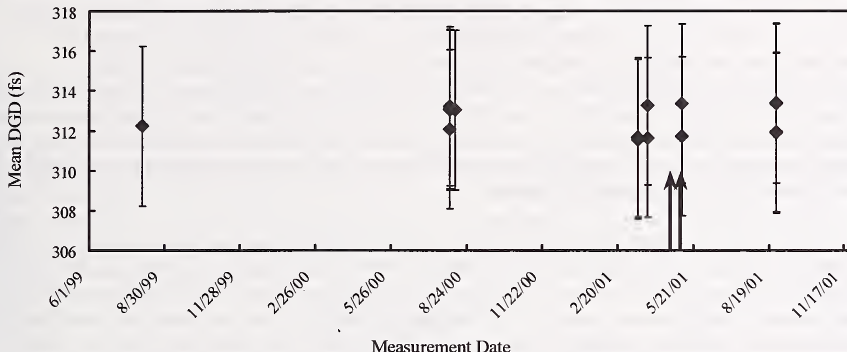

Figure 3 Control chart for SRM 2538 artifact (SN001) showing stability well within the expanded uncertainty (error bars). Vertical arrows indicate two separate dates when the artifact was temperature cycled twice from 0 °C to 50 °C.

Internal Fiber Bend Radius

The fiber leads internal to the device have been assembled to minimize bend-induced birefringence. The bend radius is kept greater than 3.5 cm (except for one 90° bend with a ~2 cm radius). Stray sources of PMD such as fiber bend birefringence would increase the amount of polarization-mode coupling in the device, allow the possibility of environmental instability, and interfere with the assumption that the majority of the spectral dependence of the DGD was due to the quartz plate. The fiber loops inside the artifact are secured to the case to prevent their motion when the artifact is moved.

3. Certification Value

NIST certifies the artifact for wavelength-averaged DGD, $\langle \Delta\tau \rangle_{\lambda_1-\lambda_2}$, also referred to here as "mean DGD", where

$$\langle \Delta\tau \rangle_{\lambda_1-\lambda_2} = \frac{\int_{\lambda_1}^{\lambda_2} \Delta\tau(\lambda) d\lambda}{\lambda_2 - \lambda_1}, \quad (1)$$

$\Delta\tau(\lambda)$ is the instantaneous DGD at wavelength λ, and λ_1 and λ_2 respectively represent the lower and upper bounds of the wavelength range over which the DGD is averaged. For the certified values reported in the SRM Certificate, this integral is approximated as a summation. We provide certification values of mean DGD over the range 1250 nm to 1650 nm and a "high-

accuracy" value averaged from approximately 1480 nm to 1570 nm. The certification procedure and associated uncertainties are described in detail in Sections 4 and 5.

4. Certifying Measurements

Measurement Details

The certified mean DGD values reported in the Certificate are based on measurements using the Jones Matrix Eigenanalysis technique. The NIST JME system [3] is capable of measuring DGD over a wavelength range of approximately1480 nm to 1570 nm. The estimate of mean DGD outside this range is found by using the JME result of mean DGD over this measurable wavelength range combined with an estimate of the dispersion of birefringence of quartz over the extended wavelength range. This extrapolation is supported (validated) with measurements made by the Fixed-Analyzer (FA) technique, sometimes called "Wavelength Scanning." The FA method is able to measure mean DGD over a 1250 nm to 1650 nm wavelength range and adds confidence to the extrapolated JME results.

The JME method is a polarimetric technique to measure differential group delay. A brief description follows. First, the Jones transfer matrix of the device under test is measured at two adjacent wavelengths. This is done by launching three different linear polarization states of light into the device under test and measuring the output Stokes vector for each launched state. This information is sufficient to determine the Jones matrix of the device under test. The two Jones matrices at adjacent wavelengths are then used to estimate the local optical frequency derivative of the Jones transfer matrix. This is then used to give the wavelength-dependent DGD of the device under test. This process is discussed in detail in Reference [1], and the NIST implementation of this technique is described in Reference [3] (this paper is included here as Appendix C).

The NIST JME system used in these measurements operates over a wavelength range of approximately 1480 nm to 1570 nm (limited by the range of the tunable laser). In certifying the artifacts, mean DGD is measured over this range by use of several different wavelength step sizes. Step size $\Delta\lambda$ is chosen subject to the requirement that the PMD-induced polarization state change is not large enough to cause aliasing. This is ensured by restricting the product of mean DGD and bandwidth such that $\Delta\tau\Delta\lambda<4$ ($\Delta\tau$ in ps and $\Delta\lambda$ in nm) [4]. Several scans of DGD are made over the nominally 1480 nm to 1570 nm wavelength range, with step sizes ranging from 2.5 nm to 10 nm. The varied step sizes allow us to verify that we are not biasing our measurement by aliasing (due to overly coarse sampling). Following Reference [5] we sampled with interleaved data points (multiple scans with the same step size but offset in wavelength) to average noise due to multiple reflections.

The mean DGD can be estimated outside of the wavelength range of the JME measurement if two conditions are met:

1. The group birefringence of quartz $\Delta n_g(\lambda)$ (defined in Appendix D) must be known over the full wavelength range of interest.
2. The PMD of the quartz plate dominates other sources of PMD within the artifact.

Condition 1 is met by using literature values of phase birefringence for quartz (as described later). Condition 2 is met since the extraneous sources of PMD provide at most a few

femtoseconds of DGD in comparison to the ~300 fs due to the quartz plate. The following description of the extrapolation of mean DGD to other wavelengths assumes that these two conditions are met.

The mean DGD of this artifact (averaged over some wavelength range from λ_1 to λ_2) can be expressed as

$$\langle \Delta\tau \rangle_{\lambda_1-\lambda_2} = \frac{\int_{\lambda_1}^{\lambda_2} \frac{\Delta n_g(\lambda)\, L_{\mathrm{eff}}}{c} d\lambda}{\lambda_2 - \lambda_1} = \frac{L_{\mathrm{eff}}}{c} \frac{\int_{\lambda_1}^{\lambda_2} \Delta n_g(\lambda)\, d\lambda}{\lambda_2 - \lambda_1} = \frac{L_{\mathrm{eff}}}{c} \langle \Delta n_g(\lambda) \rangle_{\lambda_1-\lambda_2}, \quad (2)$$

where L_{eff} is the "characteristic length." This is merely the effective physical length of the quartz crystal, slightly different from the actual physical length of the crystal due to any small degree of mode-coupling, small birefringence values that may be in other elements of the artifact (fiber leads, lenses etc.), stresses in the quartz itself, or the intentional waveplate tilt. c is the speed of light in vacuum. The quantity L_{eff}/c is given (from Eq.(2)) to be

$$\frac{L_{\mathrm{eff}}}{c} = \frac{\langle \Delta\tau(\lambda) \rangle_{\lambda_1-\lambda_2}}{\langle \Delta n_g(\lambda) \rangle_{\lambda_1-\lambda_2}}. \quad (3)$$

This quantity is independent of wavelength, and so the particular wavelength range for the averages on the right-hand side of Eq.(3) is unimportant. So, we can also express this as

$$\frac{L_{\mathrm{eff}}}{c} = \frac{\langle \Delta\tau(\lambda) \rangle_{\lambda_a-\lambda_b}}{\langle \Delta n_g(\lambda) \rangle_{\lambda_a-\lambda_b}}. \quad (4)$$

Substituting this expression for L_{eff}/c back into Eq.(2) gives

$$\langle \Delta\tau \rangle_{\lambda_1-\lambda_2} = \frac{\langle \Delta\tau(\lambda) \rangle_{\lambda_a-\lambda_b}}{\langle \Delta n_g(\lambda) \rangle_{\lambda_a-\lambda_b}} \langle \Delta n_g(\lambda) \rangle_{\lambda_1-\lambda_2}. \quad (5)$$

Eq. (5) demonstrates that the mean DGD over the wavelength range λ_1 to λ_2 can be expressed in terms of the mean DGD measured over a different wavelength range λ_a to λ_b, as long as the average group birefringence is known over both wavelength ranges. Practically, this allows us to carefully measure the mean DGD using the JME system over a range of $\lambda_a \sim 1480$ nm to $\lambda_b \sim 1570$ nm, and then using published values of the birefringence of quartz to extrapolate that value to any other wavelength range λ_1 to λ_2, as long as we have birefringence data for quartz over that range.

Our estimate of Δn_g comes from literature values of the phase birefringence Δn of quartz and is described in detail in Appendix D. We used published estimates of Δn over a window from 900 nm to 2000 nm. However, we do not report certified values of mean DGD over this entire wavelength range. We limit the wavelength range of certification to the region where we are able

to perform validating measures using the Fixed-Analyzer technique. This technique is described in general in Reference [6]. Our FA system can measure $\langle\Delta\tau\rangle$ within the 1250 nm to 1650 nm window. Our particular implementation of this technique and uncertainty estimates are given in Appendix B.

Wavelength Measurement Ranges

We report certified values of $\langle\Delta\tau\rangle$ for any averaging range within the 1250 nm to 1650 nm window, as long as the averaging span is at least 50 nm wide. If we denote the start and stop wavelengths for the DGD average as λ_1 and λ_2, respectively, these constraints can be summarized as

$$\begin{aligned} &\lambda_2 - \lambda_1 \geq 50\,\text{nm}, \\ &1250\,\text{nm} \leq \lambda_1 \leq 1600\,\text{nm}, \\ &1300\,\text{nm} \leq \lambda_2 \leq 1650\,\text{nm}. \end{aligned} \qquad (6)$$

The 50 nm minimum span requirement arises due to multiple reflections that develop in some of the artifacts. These reflections induce a periodic ripple in the DGD as a function of wavelength, and the error in mean DGD due to these ripples tends toward zero as the wavelength range of the DGD average is increased. We have found that averaging over at least a 50 nm span reduces this uncertainty to a negligible level. The upper boundary on λ_2 and the lower boundary on λ_1 come from the range of our FA measurement. We certify measurements of the mean DGD only over wavelengths we were able to verify experimentally with our FA technique. Certified values of mean DGD within this wavelength range are provided as a "look-up" table in the Certificate (Appendix A).

We also certify a "high-accuracy" value of the mean DGD over the wavelength range of approximately 1480 nm to 1570 nm. This value is measured using only the JME technique (with no need for extrapolation. This simplification in measurement procedures allows for a lower uncertainty).

5. Uncertainty Analysis

To simplify discussion of the uncertainty analysis, it is broken into two parts. First is the uncertainty associated with the JME measurement of mean DGD over the nominally 1480 nm to 1570 nm range. This constitutes the total uncertainty of the "high-accuracy" value. Second is a description of the uncertainty of the mean DGD values that come from the wavelength extrapolation of this "high-accuracy" value.

5.1 "High-Accuracy" Value

From Reference [3], we estimate the NIST JME system to yield a standard uncertainty of 1.7 fs on artifacts of nominally 500 fs mean DGD. (The exact value in Reference [3] differs by ~0.1 fs due to a difference in fiber leads.) The uncertainty of the JME measurement is dominated by the effect of birefringence in the system's fiber leads, but also includes a contribution due to random uncertainty, which is slightly different for each artifact. As an example, JME measurements of the mean DGD of a 312 fs artifact over the approximately 1480 nm to 1570 nm range yielded a standard deviation of the mean (SDOM) of 0.22 fs. The combined standard uncertainty of this measurement is the quadrature sum of these two values. The SRM Certificate report expanded

uncertainty (combined standard uncertainty multiplied by a coverage factor of $k = 2$ [7]). This yields 3.4 fs with an approximate 95 % confidence interval, as illustrated in Table 2.

Table 2. Summary of measurement uncertainty for a particular 312 fs artifact over the "high-accuracy" ~1480 nm to 1570 nm wavelength range.

Uncertainty Source	Standard Uncertainty (fs)
JME measurement system	1.7
Measurement repeatability (SDOM)	0.22
Combined standard uncertainty, u_c	1.7
Expanded uncertainty, $U=2u_c$	**3.4**

5.2 Wavelength-Extrapolated Range

For an extended wavelength range estimate of $\langle\Delta\tau\rangle$, a propagation-of-uncertainty expression for Eq.(5) yields

$$U^2(\langle\Delta\tau\rangle_{\lambda_1-\lambda_2}) \approx (\langle\Delta\tau\rangle_{\lambda_1-\lambda_2})^2\left(\left(\frac{U(\langle\Delta n_g\rangle_{\lambda_1-\lambda_2})}{\langle\Delta n_g\rangle_{\lambda_1-\lambda_2}}\right)^2+\left(\frac{U(\langle\Delta n_g\rangle_{\lambda_a-\lambda_b})}{\langle\Delta n_g\rangle_{\lambda_a-\lambda_b}}\right)^2+\left(\frac{U(\langle\Delta\tau\rangle_{\lambda_a-\lambda_b})}{\langle\Delta\tau\rangle_{\lambda_a-\lambda_b}}\right)^2\right), \quad (7)$$

where $U(x)$ represents the uncertainty of the value x. The first two uncertainty terms are, respectively, the uncertainty of the mean of the estimated group birefringence Δn_g evaluated over the extrapolated wavelength range λ_1 to λ_2, and this same uncertainty over the "narrow" range λ_a to λ_b (approximately 1480 nm to 1570 nm) where the JME measurement was performed. These two terms account for the uncertainty due to the extrapolation of the measured mean DGD values to wavelength ranges not directly measured using the JME technique. The third term is the uncertainty from the JME measurement of mean DGD over the 1480 nm to 1570 nm range as described in Section 5.1. For easy reference, the uncertainty components of Eq.(8) are given the following names:

$$U^2(\langle\Delta\tau\rangle_{\lambda_1-\lambda_2}) = U^2(\Delta\tau,\text{ext}) \approx U^2(\Delta n_g,\text{ext}) + U^2(\Delta n_g,\text{narrow}) + U^2(\Delta\tau,\text{narrow}). \quad (8)$$

The "JME uncertainty", $U(\Delta\tau,\text{narrow})$, is the normalized uncertainty over the short-wavelength average of $\Delta\tau$, as discussed in Section 5.1. A typical value for the 312 fs artifact is

$$U(\Delta\tau,\text{narrow}) = (\langle\Delta\tau\rangle_{1271.5-1638.6})\left(\frac{U(\langle\Delta\tau\rangle_{1481.25-1568.25})}{\langle\Delta\tau\rangle_{1481.25-1568.25}}\right) = 1.7\,\text{fs}. \quad (9)$$

We will now describe our estimate of the uncertainty of $\langle\Delta n_g\rangle$. As mentioned in Appendix D, the estimate of Δn_g comes from the differentiation of a third-order polynomial fit to published values of Δn (phase birefringence) for quartz. Therefore, the uncertainty of Δn_g must take into account the uncertainty of the published Δn data as well as the uncertainty incurred by the curve-fitting and extrapolation process.

Appendix D illustrates how published Δn values were used to generate Δn_g values. In order to allow for possible sample-to-sample variation of Δn_g, we derive an uncertainty based on the variation of the literature values of Δn. The $\Delta n(\lambda)$ values from [8] were fit to a third-order polynomial using a least-squares technique. The residual differences between the Reference [8] $\Delta n(\lambda)$ values predicted by this fit and the $\Delta n(\lambda)$ values reported in reference [9] were calculated. This gave us a measure of the disagreement between Δn values from the two references. For the 900-2000 nm data range used, this residual value had a standard deviation of 0.0000116. We also verified this uncertainty experimentally in Appendix B of Reference [3]. This uncertainty was used with the covariance matrix [10] of the fitted coefficients to Δn to give an uncertainty on the polynomial coefficients from Eq. (D2). This was used with a propagation of uncertainty of the expression for Δn_g (Eq. D3) to yield a wavelength-dependent uncertainty of Δn_g.

The uncertainty of the wavelength-averaged group birefringence $\langle \Delta n_g \rangle_{\lambda_1-\lambda_2}$ is based on a curve-fit to individual $\Delta n_g(\lambda)$ values, and we must assume that the Δn_g values at different wavelengths are correlated. The worst-case uncertainty would be for positive, perfect correlation in these values. This would mean that the uncertainty of the wavelength-averaged group birefringence is equal to the average of the uncertainty of the group birefringence at each wavelength

$$U(\langle \Delta n_g \rangle_{\lambda_1-\lambda_2}) = \langle U(\Delta n_g) \rangle_{\lambda_1-\lambda_2}. \qquad (10)$$

So, the uncertainty contributions for $U(\Delta n_g,\text{extrapolated})$ and $U(\Delta n_g,\text{narrow})$ are estimated by averaging the individual uncertainty estimates of $\Delta n_g(\lambda)$ over the appropriate wavelength ranges. Averaging over a broader wavelength range does not necessarily reduce the $U(\Delta n_g)$ estimate.

As an example of the magnitudes of these various uncertainty components, a 312 fs artifact yields the uncertainties

$$U(\Delta n_g, \text{narrow}) = (\langle \Delta \tau \rangle_{1271.5-1638.6}) \left(\frac{U(\langle \Delta n_g \rangle_{1481.25-1568.25})}{\langle \Delta n_g \rangle_{1481.25-1568.25}} \right) = 0.86 \text{ fs} \qquad (11)$$

and

$$U(\Delta n_g, ext) = (\langle \Delta \tau \rangle_{1271.5-1638.6}) \left(\frac{U(\langle \Delta n_g \rangle_{1271.5-1638.6})}{\langle \Delta n_g \rangle_{1271.5-1638.6}} \right) = 0.82 \text{ fs}. \qquad (12)$$

Because we report the mean DGD for so many possible wavelength ranges (Table 2 of the SRM Certificate, Appendix A), we take a simplifying approach to the uncertainty. We report one worst-case uncertainty for $\langle \Delta\tau \rangle$, which is applicable to all possible wavelength ranges within the constraints of Eqs.(6) ("one size fits all").

We arrived at this worst-case estimate as follows. The uncertainty of $U(\Delta\tau,\text{narrow})$ is as reported in Section 5.1. The uncertainty of $U(\Delta n_g,\text{narrow})$ is the same as described above. The third uncertainty component of Eq.(8), $U(\Delta n_g,\text{ext})$, is the average of the group birefringence uncertainty over the extrapolated wavelength range. In order to simplify the estimate of this last term, we use the largest value of the $\langle \Delta n_g \rangle$ uncertainty that we found for a variety of wavelength ranges within the constraints of Eqs (6). Table D2 shows the $\langle \Delta n_g \rangle$ uncertainties incurred for

these ranges, with the worst-case being 0.000027 over the range 1450 nm to 1500 nm. Normalizing this value to the mean group birefringence and multiplying by the mean DGD (from Eq.(7)) over this wavelength range will give the worst-case value for $U(\Delta n_g, \text{ext})$. For our 312 fs artifact example, the worst-case value for $U(\Delta n_g, \text{ext})$ turns out to be 0.89 fs, only slightly different from the specific example of Eq. (12). This verifies that using one uncertainty value for all the valid wavelength ranges is not significantly different from reporting each uncertainty individually.

The quadrature sum of the three terms in Eq. (8) yields the uncertainty estimate for the mean DGD measurement over the extrapolated range. Since this requires an estimate of mean DGD over a range containing wavelengths where no JME measurements were actually made, we performed a validating Fixed Analyzer measurement over the specified wavelength range (to verify our extrapolated estimate). We use the results of this comparison only to better estimate the uncertainty on the JME measured result (not to modify the result itself). The total uncertainty on the extrapolation then comes from the JME uncertainty of Eq. (8) added in quadrature with the uncertainty of bias between the JME extrapolation and the FA measurements of the artifact over the extrapolated range. This approach is based on the "BOB" solution to the two-method problem described in [11] and requires the assumption that the true value of mean DGD be bounded by the JME and Fixed-Analyzer results. In the course of this work, we have evaluated the most significant sources of FA uncertainty and include a description in Appendix B for completeness.

At least one validating FA measurement is made over the ~1250 nm to 1650 nm wavelength range. As described in Appendix B, this FA measurement yields the mean DGD over the entire measurement range and the mean DGD over a 50 nm to 100 nm range at each end of the wide scan. This yields three FA-based estimates of mean DGD. These are compared to extrapolations of the JME-based measurement over the same three wavelength ranges. The uncertainty of bias between the JME and FA measurements for an extrapolated wavelength range of approximately 1250 to 1650 nm, for all of the artifacts measured, is added in quadrature to the uncertainty estimated from Eq. (8).

Then, we add, in quadrature, $U(\Delta n_g, \text{narrow})$, $U(\Delta n_g, \text{narrow})$, $U(\Delta\tau, \text{narrow})$, and the bias estimate from the comparative FA measurements. For the 312 fs artifact example, this yields an expanded uncertainty ("$k = 2$" coverage factor [7]) of 4.2 fs, as illustrated in Table 3.

Table 3. Summary of measurement uncertainty for a particular 312 fs artifact over any extrapolated wavelength range (subject to constraints of Eqs. (6)).

Uncertainty Source	Standard Uncertainty (fs)
"Narrow" wavelength range measurement, $U(\Delta\tau, \text{narrow})$	1.7
Δn_g estimate ("Narrow" range), $U(\Delta n_g, \text{narrow})$	0.86
Δn_g estimate (extrapolated range), $U(\Delta n_g, \text{ext})$	0.89
FA validation	0.12
Combined standard uncertainty, u_c	2.1
Expanded uncertainty, $U=2u_c$	**4.2**

For each artifact certified, we perform many (~500) JME measurements of DGD(λ) over the

~1480 nm to 1570 nm range with the artifact moved, the leads manipulated, and the power turned off for several hours and back on at least once between the measurement sets. In between these measurements, each device is also temperature cycled from 0 °C to 50 °C at least twice (as described in Section 2). These DGD results are averaged to arrive at the estimated mean DGD values.

Fig. 4 illustrates typical agreement between the two techniques. The difference in mean DGD at each wavelength is plotted for nine SRM 2538 artifacts measured using JME (plus extrapolation) and FA. The average of the discrepancy between the two measurements plus the "prediction error" (standard deviation of the mean of the discrepancy) for the ~1250 nm to 1650 nm wavelength range yields the estimate of the uncertainty of bias. This turned out to be a small value of 0.4 fs, which gives a standard uncertainty of 0.4 fs / $\sqrt{12}$ or 0.12 fs (assuming a uniformly distributed error [7]). This quantity is negligible when added in quadrature with the uncertainty result of Eq. (9). As shown in Table 3, our 312 fs example artifact yielded a combined standard uncertainty for any wavelength range within the constraints of Eqs. (6) of 2.1 fs. Doubling this value gives the expanded uncertainty of 4.2 fs, as would be reported in the certificate with a "$k = 2$" coverage factor [7], yielding an approximately 95 % confidence interval.

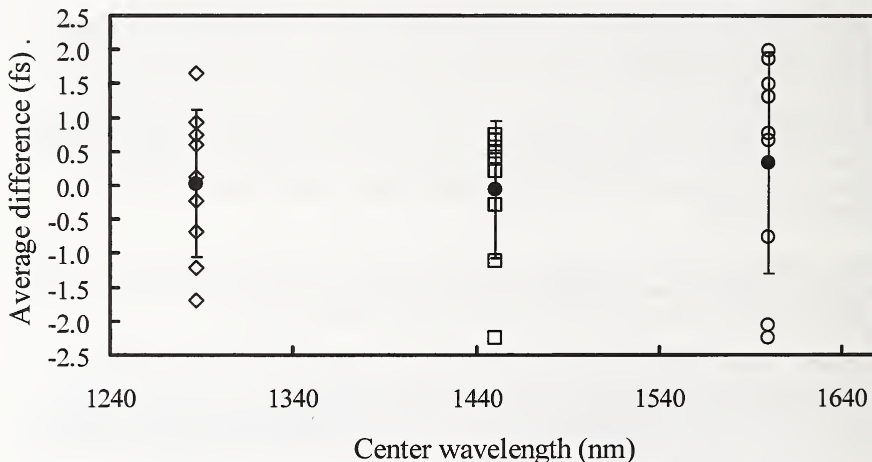

Figure 4. Difference between JME and Fixed Analyzer measurements of mean DGD in 9 artifacts of SRM 2538. Open symbols represent data for each artifact. Filled circles are the mean; error bar is one standard deviation.

6. References:

[1] B.L. Heffner, "Automated Measurement of Polarization Mode Dispersion Using Jones Matrix Eigenanalysis," *Photonics Technology Letters* **4**, 1066-1069 (1992).

[2] Shelley M. Etzel, A.H. Rose, and C.M. Wang, "Dispersion of the temperature dependence of the retardance in SiO_2 and MgF_2," *Applied Optics* **39**, 5796-5800 (2000).

[3] P.A. Williams, "Rotating Waveplate Stokes Polarimeter for Differential Group Delay Measurements of Polarization-Mode Dispersion," *Applied Optics* **38**, 6508-6515 (1999).

[4] Dennis Derickson, Ed., *Fiber optic test and measurement*, p. 504, Prentice Hall, New Jersey (1998).

[5] P.A. Williams, "Mode-coupled artifact standard for polarization-mode dispersion: design, assembly, and implementation," *Applied Optics* **38**, 6498-6507 (1999).

[6] Dennis Derickson, Ed., *Fiber optic test and measurement*, p. 495, Prentice Hall, New Jersey (1998).

[7] B.N. Taylor and C.E. Kuyatt, Eds.; "Guidelines for evaluating and expressing the uncertainty of NIST measurement results," National Institute of Standards and Technology, Tech. Note 1297, 1994.

[8] John H. Shields and Joseph W. Ellis, "Dispersion of birefringence of quartz in the near infrared," Journal of the Optical Society of America 46, 263-265 (1956).

[9] William L. Wolfe and George J. Zissis Eds, *The Infrared Handbook* (Environmental Research Institute of Michigan, Ann Arbor, 1985), p. 7-57.

[10] F.A. Graybill and H.K. Iyer, *Regression Analysis: Concepts and Applications*, (Belmont, CA: Wadsworth, 1994), p. 263.

[11] M.S. Levenson, D.L. Banks, K.R. Eberhardt, L.M. Gill, W.F.Guthrie, H.K. Liu, M.G. Vangel, J.H. Yen, and N.F. Zhang, "An Approach to Combining Results From Multiple Methods Motivated by the ISO GUM," *Journal of Research of the National Institute of Standards and Technology* **105**, 571-579 (2000).

[12] P.A. Williams and C.M. Wang, "Corrections to Fixed Analyzer Measurements of Polarization Mode Dispersion," *Journal of Lightwave Technology* **16**, 534-541 (1998).

[13] Sasada, H. and Yamada, K., "Calibration Lines of HCN in the 1.5-μm region," *Applied Optics* **29**, 3535-3547 (1990).

[14] Kinpui Chan, Hiromasa Ito, and Humio Inaba, "Absorption measurement of $\nu_2 + 2\nu_3$ band of CH_4 at 1.33 μm using an InGaAsP light emitting diode," *Applied Optics* **22**, 3802-3804 (1983).

[15] J.D. Jackson, Classical Electrodynamics, (Wiley, New York, 1975), pp. 299-303.

National Institute of Standards & Technology

Certificate of Analysis

Standard Reference Material® 2538

Polarization-Mode Dispersion (Non-Mode-Coupled)

Serial No.: ___

This Standard Reference Material (SRM) is intended for use for the calibration of polarization-mode dispersion (PMD) measurements on non-mode-coupled devices. Certified data apply only to the artifact with the serial number shown above.

Expiration of Certification: The SRM will remain in certification indefinitely, provided the cleaning and storage instructions are followed and the housing is not opened. A sudden increase in insertion loss or the sudden appearance of ripples in the DGD spectrum are indications that something has changed in the device. If this occurs, carefully clean the connectors, examining the fiber pigtails to be attached to the SRM, and repeat the measurement.

Scope of Use: This SRM has been characterized for wavelength-averaged differential group delay (mean DGD), and this certificate supplies certified values over any wavelength range subject to the wavelength constraints listed.

In principle, the artifact (SRM) is certified for measurement by all PMD measurement techniques that give wavelength-averaged (mean) DGD over an allowed wavelength range. However, care must be taken as to how the DGD is averaged over the measurement range. **The certification contained in this document pertains to a uniformly weighted wavelength average of DGD.** For example, when low-coherence interferometry or the Fourier-Transformed Fixed Analyzer measurement techniques are used, the spectral shape of the source can weight the averaged DGD toward the wavelength where the source has the most power. Therefore, if these techniques are used without wavelength normalization, the DGD over a wavelength range where the source intensity is low will be weighted less than the DGD at a wavelength with high source intensity. The user should be aware of this when measuring this artifact with such techniques in order to properly interpret uncertainty statements.

Certified Values and Uncertainties: The mean DGD measurements were performed using the NIST Jones Matrix Eigenanalysis system [1], and verified with a Fixed Analyzer (Wavelength Scanning) measurement. This certificate reports mean DGD averaged over any range of wavelength within the 1250 nm to 1650 nm window subject to a 50 nm minimum span width. These wavelength range constraints are summarized as

$$\begin{aligned} &\lambda_2 - \lambda_1 \geq 50 \text{ nm} \\ &1250 \text{ nm} \leq \lambda_1 \leq 1600 \text{ nm} \\ &1300 \text{ nm} \leq \lambda_2 \leq 1650 \text{ nm} \end{aligned} \tag{1}$$

where λ_1 and λ_2 are, respectively, the minimum and maximum wavelengths of the averaging range. The certified values of mean DGD are found in Table 1. Given a start wavelength λ_1 and a stop wavelength λ_2, this table reports the mean DGD of the artifact for averaging between these two wavelengths. Note that wavelengths are resolved only to 5 nm as this is sufficient for the DGD resolution provided. To use the table, find the nearest start wavelength (within 5 nm) on the top row and nearest stop wavelength (within 5 nm) on the left column. The intersection point of the row and column defined by these two wavelengths gives the certified mean DGD over the selected wavelength range. The associated uncertainty, given at the top of Table 1, represents a coverage factor of k=2, yielding an approximate 95 % confidence interval.

The support aspects involved with the certification and issuance of this SRM were coordinated through the NIST Standard Reference Materials Group by J.W.L. Thomas.

Gordon Day, Chief
Optoelectronics Division

John Rumble, Jr., Chief
Measurement Services Division

Gaithersburg, MD 20899
Certificate Issue Date: 8 July 2002

The research and development effort leading to this SRM included contributions from the following NIST personnel: S.M. Etzel, J.D. Kofler, and P.A. Williams (NIST Optoelectronics Division), and C.M. Wang (NIST Statistical Engineering Division). Questions regarding this device should be addressed to Paul Williams at telephone (303) 497-3805 or email paul.williams@nist.gov.

INSTRUCTIONS FOR USE

The SRM 2538 unit is a pigtailed quartz plate with FC/APC style connectors (2.15 mm “wide key”). The temperature of the quartz plate is actively controlled to ensure a stable mean DGD value. This unit requires an AC power source (115 V, 60 Hz).

The SRM is a delicate optical instrument and should be handled carefully. Damage can easily occur if the device is dropped or jarred. The housing should not be opened, and the optical connectors should be cleaned carefully before each connection. When making connections to the SRM, use high quality FC/APC connectors (2.15 mm “wide key”). The cleanliness of the connectors is important. Use a dust free and residue-free air source and a commercial fiber endface cleaner before every connection. If such a cleaner is not available, then lens paper wetted with reagent-grade isopropyl alcohol can be used to wipe the ferrule endface and the air source used to dry the connector.

When not in use, the device should be stored at a temperature from 15 °C to 30 °C in a clean, dry environment.

Table 1. Certified value of mean DGD (fs) for SRM 2538 serial number ___ averaged over the wavelength range from “start wavelength” to “stop wavelength”. **Expanded uncertainty (95 % confidence interval) for any value in this table is x.x fs.**

stop wavelength (nm) ↓ / start wavelength (nm) →	1250	1255	1260	1265	1270	1275	1280	1285	1290	1295	1300	1305	1310	1315	1320	1325	1330	1335	1340	1345
1650	xxx.x	xxx.x	xxx.x	xxx.x	xxx.x	xxx.x	xxx.x	xxx.x	xxx.x	xxx.x	xxx.x	xxx.x	xxx.x	xxx.x	xxx.x	xxx.x	xxx.x	xxx.x	xxx.x	xxx.x
1645	xxx.x	xxx.x	xxx.x	xxx.x	xxx.x	xxx.x	xxx.x	xxx.x	xxx.x	xxx.x	xxx.x	xxx.x	xxx.x	xxx.x	xxx.x	xxx.x	xxx.x	xxx.x	xxx.x	xxx.x
1640	xxx.x	xxx.x	xxx.x	xxx.x	xxx.x	xxx.x	xxx.x	xxx.x	xxx.x	xxx.x	xxx.x	xxx.x	xxx.x	xxx.x	xxx.x	xxx.x	xxx.x	xxx.x	xxx.x	xxx.x
1635	xxx.x	xxx.x	xxx.x	xxx.x	xxx.x	xxx.x	xxx.x	xxx.x	xxx.x	xxx.x	xxx.x	xxx.x	xxx.x	xxx.x	xxx.x	xxx.x	xxx.x	xxx.x	xxx.x	xxx.x
1630	xxx.x	xxx.x	xxx.x	xxx.x	xxx.x	xxx.x	xxx.x	xxx.x	xxx.x	xxx.x	xxx.x	xxx.x	xxx.x	xxx.x	xxx.x	xxx.x	xxx.x	xxx.x	xxx.x	xxx.x
1625	xxx.x	xxx.x	xxx.x	xxx.x	xxx.x	xxx.x	xxx.x	xxx.x	xxx.x	xxx.x	xxx.x	xxx.x	xxx.x	xxx.x	xxx.x	xxx.x	xxx.x	xxx.x	xxx.x	xxx.x
1620	xxx.x	xxx.x	xxx.x	xxx.x	xxx.x	xxx.x	xxx.x	xxx.x	xxx.x	xxx.x	xxx.x	xxx.x	xxx.x	xxx.x	xxx.x	xxx.x	xxx.x	xxx.x	xxx.x	xxx.x
1615	xxx.x	xxx.x	xxx.x	xxx.x	xxx.x	xxx.x	xxx.x	xxx.x	xxx.x	xxx.x	xxx.x	xxx.x	xxx.x	xxx.x	xxx.x	xxx.x	xxx.x	xxx.x	xxx.x	xxx.x
1610	xxx.x	xxx.x	xxx.x	xxx.x	xxx.x	xxx.x	xxx.x	xxx.x	xxx.x	xxx.x	xxx.x	xxx.x	xxx.x	xxx.x	xxx.x	xxx.x	xxx.x	xxx.x	xxx.x	xxx.x
1605	xxx.x	xxx.x	xxx.x	xxx.x	xxx.x	xxx.x	xxx.x	xxx.x	xxx.x	xxx.x	xxx.x	xxx.x	xxx.x	xxx.x	xxx.x	xxx.x	xxx.x	xxx.x	xxx.x	xxx.x
1600	xxx.x	xxx.x	xxx.x	xxx.x	xxx.x	xxx.x	xxx.x	xxx.x	xxx.x	xxx.x	xxx.x	xxx.x	xxx.x	xxx.x	xxx.x	xxx.x	xxx.x	xxx.x	xxx.x	xxx.x
1595	xxx.x	xxx.x	xxx.x	xxx.x	xxx.x	xxx.x	xxx.x	xxx.x	xxx.x	xxx.x	xxx.x	xxx.x	xxx.x	xxx.x	xxx.x	xxx.x	xxx.x	xxx.x	xxx.x	xxx.x
1590	xxx.x	xxx.x	xxx.x	xxx.x	xxx.x	xxx.x	xxx.x	xxx.x	xxx.x	xxx.x	xxx.x	xxx.x	xxx.x	xxx.x	xxx.x	xxx.x	xxx.x	xxx.x	xxx.x	xxx.x
1585	xxx.x	xxx.x	xxx.x	xxx.x	xxx.x	xxx.x	xxx.x	xxx.x	xxx.x	xxx.x	xxx.x	xxx.x	xxx.x	xxx.x	xxx.x	xxx.x	xxx.x	xxx.x	xxx.x	xxx.x
1580	xxx.x	xxx.x	xxx.x	xxx.x	xxx.x	xxx.x	xxx.x	xxx.x	xxx.x	xxx.x	xxx.x	xxx.x	xxx.x	xxx.x	xxx.x	xxx.x	xxx.x	xxx.x	xxx.x	xxx.x
1575	xxx.x	xxx.x	xxx.x	xxx.x	xxx.x	xxx.x	xxx.x	xxx.x	xxx.x	xxx.x	xxx.x	xxx.x	xxx.x	xxx.x	xxx.x	xxx.x	xxx.x	xxx.x	xxx.x	xxx.x
1570	xxx.x	xxx.x	xxx.x	xxx.x	xxx.x	xxx.x	xxx.x	xxx.x	xxx.x	xxx.x	xxx.x	xxx.x	xxx.x	xxx.x	xxx.x	xxx.x	xxx.x	xxx.x	xxx.x	xxx.x
1565	xxx.x	xxx.x	xxx.x	xxx.x	xxx.x	xxx.x	xxx.x	xxx.x	xxx.x	xxx.x	xxx.x	xxx.x	xxx.x	xxx.x	xxx.x	xxx.x	xxx.x	xxx.x	xxx.x	xxx.x
1560	xxx.x	xxx.x	xxx.x	xxx.x	xxx.x	xxx.x	xxx.x	xxx.x	xxx.x	xxx.x	xxx.x	xxx.x	xxx.x	xxx.x	xxx.x	xxx.x	xxx.x	xxx.x	xxx.x	xxx.x
1555	xxx.x	xxx.x	xxx.x	xxx.x	xxx.x	xxx.x	xxx.x	xxx.x	xxx.x	xxx.x	xxx.x	xxx.x	xxx.x	xxx.x	xxx.x	xxx.x	xxx.x	xxx.x	xxx.x	xxx.x
1550	xxx.x	xxx.x	xxx.x	xxx.x	xxx.x	xxx.x	xxx.x	xxx.x	xxx.x	xxx.x	xxx.x	xxx.x	xxx.x	xxx.x	xxx.x	xxx.x	xxx.x	xxx.x	xxx.x	xxx.x
1545	xxx.x	xxx.x	xxx.x	xxx.x	xxx.x	xxx.x	xxx.x	xxx.x	xxx.x	xxx.x	xxx.x	xxx.x	xxx.x	xxx.x	xxx.x	xxx.x	xxx.x	xxx.x	xxx.x	xxx.x
1540	xxx.x	xxx.x	xxx.x	xxx.x	xxx.x	xxx.x	xxx.x	xxx.x	xxx.x	xxx.x	xxx.x	xxx.x	xxx.x	xxx.x	xxx.x	xxx.x	xxx.x	xxx.x	xxx.x	xxx.x
1535	xxx.x	xxx.x	xxx.x	xxx.x	xxx.x	xxx.x	xxx.x	xxx.x	xxx.x	xxx.x	xxx.x	xxx.x	xxx.x	xxx.x	xxx.x	xxx.x	xxx.x	xxx.x	xxx.x	xxx.x
1530	xxx.x	xxx.x	xxx.x	xxx.x	xxx.x	xxx.x	xxx.x	xxx.x	xxx.x	xxx.x	xxx.x	xxx.x	xxx.x	xxx.x	xxx.x	xxx.x	xxx.x	xxx.x	xxx.x	xxx.x
1525	xxx.x	xxx.x	xxx.x	xxx.x	xxx.x	xxx.x	xxx.x	xxx.x	xxx.x	xxx.x	xxx.x	xxx.x	xxx.x	xxx.x	xxx.x	xxx.x	xxx.x	xxx.x	xxx.x	xxx.x
1520	xxx.x	xxx.x	xxx.x	xxx.x	xxx.x	xxx.x	xxx.x	xxx.x	xxx.x	xxx.x	xxx.x	xxx.x	xxx.x	xxx.x	xxx.x	xxx.x	xxx.x	xxx.x	xxx.x	xxx.x
1515	xxx.x	xxx.x	xxx.x	xxx.x	xxx.x	xxx.x	xxx.x	xxx.x	xxx.x	xxx.x	xxx.x	xxx.x	xxx.x	xxx.x	xxx.x	xxx.x	xxx.x	xxx.x	xxx.x	xxx.x
1510	xxx.x	xxx.x	xxx.x	xxx.x	xxx.x	xxx.x	xxx.x	xxx.x	xxx.x	xxx.x	xxx.x	xxx.x	xxx.x	xxx.x	xxx.x	xxx.x	xxx.x	xxx.x	xxx.x	xxx.x
1505	xxx.x	xxx.x	xxx.x	xxx.x	xxx.x	xxx.x	xxx.x	xxx.x	xxx.x	xxx.x	xxx.x	xxx.x	xxx.x	xxx.x	xxx.x	xxx.x	xxx.x	xxx.x	xxx.x	xxx.x
1500	xxx.x	xxx.x	xxx.x	xxx.x	xxx.x	xxx.x	xxx.x	xxx.x	xxx.x	xxx.x	xxx.x	xxx.x	xxx.x	xxx.x	xxx.x	xxx.x	xxx.x	xxx.x	xxx.x	xxx.x
1495	xxx.x	xxx.x	xxx.x	xxx.x	xxx.x	xxx.x	xxx.x	xxx.x	xxx.x	xxx.x	xxx.x	xxx.x	xxx.x	xxx.x	xxx.x	xxx.x	xxx.x	xxx.x	xxx.x	xxx.x
1490	xxx.x	xxx.x	xxx.x	xxx.x	xxx.x	xxx.x	xxx.x	xxx.x	xxx.x	xxx.x	xxx.x	xxx.x	xxx.x	xxx.x	xxx.x	xxx.x	xxx.x	xxx.x	xxx.x	xxx.x
1485	xxx.x	xxx.x	xxx.x	xxx.x	xxx.x	xxx.x	xxx.x	xxx.x	xxx.x	xxx.x	xxx.x	xxx.x	xxx.x	xxx.x	xxx.x	xxx.x	xxx.x	xxx.x	xxx.x	xxx.x
1480	xxx.x	xxx.x	xxx.x	xxx.x	xxx.x	xxx.x	xxx.x	xxx.x	xxx.x	xxx.x	xxx.x	xxx.x	xxx.x	xxx.x	xxx.x	xxx.x	xxx.x	xxx.x	xxx.x	xxx.x
1475	xxx.x	xxx.x	xxx.x	xxx.x	xxx.x	xxx.x	xxx.x	xxx.x	xxx.x	xxx.x	xxx.x	xxx.x	xxx.x	xxx.x	xxx.x	xxx.x	xxx.x	xxx.x	xxx.x	xxx.x
1470	xxx.x	xxx.x	xxx.x	xxx.x	xxx.x	xxx.x	xxx.x	xxx.x	xxx.x	xxx.x	xxx.x	xxx.x	xxx.x	xxx.x	xxx.x	xxx.x	xxx.x	xxx.x	xxx.x	xxx.x
1465	xxx.x	xxx.x	xxx.x	xxx.x	xxx.x	xxx.x	xxx.x	xxx.x	xxx.x	xxx.x	xxx.x	xxx.x	xxx.x	xxx.x	xxx.x	xxx.x	xxx.x	xxx.x	xxx.x	xxx.x
1460	xxx.x	xxx.x	xxx.x	xxx.x	xxx.x	xxx.x	xxx.x	xxx.x	xxx.x	xxx.x	xxx.x	xxx.x	xxx.x	xxx.x	xxx.x	xxx.x	xxx.x	xxx.x	xxx.x	xxx.x
1455	xxx.x	xxx.x	xxx.x	xxx.x	xxx.x	xxx.x	xxx.x	xxx.x	xxx.x	xxx.x	xxx.x	xxx.x	xxx.x	xxx.x	xxx.x	xxx.x	xxx.x	xxx.x	xxx.x	xxx.x
1450	xxx.x	xxx.x	xxx.x	xxx.x	xxx.x	xxx.x	xxx.x	xxx.x	xxx.x	xxx.x	xxx.x	xxx.x	xxx.x	xxx.x	xxx.x	xxx.x	xxx.x	xxx.x	xxx.x	xxx.x
1445	xxx.x	xxx.x	xxx.x	xxx.x	xxx.x	xxx.x	xxx.x	xxx.x	xxx.x	xxx.x	xxx.x	xxx.x	xxx.x	xxx.x	xxx.x	xxx.x	xxx.x	xxx.x	xxx.x	xxx.x
1440	xxx.x	xxx.x	xxx.x	xxx.x	xxx.x	xxx.x	xxx.x	xxx.x	xxx.x	xxx.x	xxx.x	xxx.x	xxx.x	xxx.x	xxx.x	xxx.x	xxx.x	xxx.x	xxx.x	xxx.x
1435	xxx.x	xxx.x	xxx.x	xxx.x	xxx.x	xxx.x	xxx.x	xxx.x	xxx.x	xxx.x	xxx.x	xxx.x	xxx.x	xxx.x	xxx.x	xxx.x	xxx.x	xxx.x	xxx.x	xxx.x
1430	xxx.x	xxx.x	xxx.x	xxx.x	xxx.x	xxx.x	xxx.x	xxx.x	xxx.x	xxx.x	xxx.x	xxx.x	xxx.x	xxx.x	xxx.x	xxx.x	xxx.x	xxx.x	xxx.x	xxx.x
1425	xxx.x	xxx.x	xxx.x	xxx.x	xxx.x	xxx.x	xxx.x	xxx.x	xxx.x	xxx.x	xxx.x	xxx.x	xxx.x	xxx.x	xxx.x	xxx.x	xxx.x	xxx.x	xxx.x	xxx.x
1420	xxx.x	xxx.x	xxx.x	xxx.x	xxx.x	xxx.x	xxx.x	xxx.x	xxx.x	xxx.x	xxx.x	xxx.x	xxx.x	xxx.x	xxx.x	xxx.x	xxx.x	xxx.x	xxx.x	xxx.x
1415	xxx.x	xxx.x	xxx.x	xxx.x	xxx.x	xxx.x	xxx.x	xxx.x	xxx.x	xxx.x	xxx.x	xxx.x	xxx.x	xxx.x	xxx.x	xxx.x	xxx.x	xxx.x	xxx.x	xxx.x
1410	xxx.x	xxx.x	xxx.x	xxx.x	xxx.x	xxx.x	xxx.x	xxx.x	xxx.x	xxx.x	xxx.x	xxx.x	xxx.x	xxx.x	xxx.x	xxx.x	xxx.x	xxx.x	xxx.x	xxx.x
1405	xxx.x	xxx.x	xxx.x	xxx.x	xxx.x	xxx.x	xxx.x	xxx.x	xxx.x	xxx.x	xxx.x	xxx.x	xxx.x	xxx.x	xxx.x	xxx.x	xxx.x	xxx.x	xxx.x	xxx.x
1400	xxx.x	xxx.x	xxx.x	xxx.x	xxx.x	xxx.x	xxx.x	xxx.x	xxx.x	xxx.x	xxx.x	xxx.x	xxx.x	xxx.x	xxx.x	xxx.x	xxx.x	xxx.x	xxx.x	xxx.x
1395	xxx.x	xxx.x	xxx.x	xxx.x	xxx.x	xxx.x	xxx.x	xxx.x	xxx.x	xxx.x	xxx.x	xxx.x	xxx.x	xxx.x	xxx.x	xxx.x	xxx.x	xxx.x	xxx.x	xxx.x
1390	xxx.x	xxx.x	xxx.x	xxx.x	xxx.x	xxx.x	xxx.x	xxx.x	xxx.x	xxx.x	xxx.x	xxx.x	xxx.x	xxx.x	xxx.x	xxx.x	xxx.x	xxx.x	xxx.x	
1385	xxx.x	xxx.x	xxx.x	xxx.x	xxx.x	xxx.x	xxx.x	xxx.x	xxx.x	xxx.x	xxx.x	xxx.x	xxx.x	xxx.x	xxx.x	xxx.x	xxx.x	xxx.x		
1380	xxx.x	xxx.x	xxx.x	xxx.x	xxx.x	xxx.x	xxx.x	xxx.x	xxx.x	xxx.x	xxx.x	xxx.x	xxx.x	xxx.x	xxx.x	xxx.x	xxx.x			
1375	xxx.x	xxx.x	xxx.x	xxx.x	xxx.x	xxx.x	xxx.x	xxx.x	xxx.x	xxx.x	xxx.x	xxx.x	xxx.x	xxx.x	xxx.x	xxx.x				
1370	xxx.x	xxx.x	xxx.x	xxx.x	xxx.x	xxx.x	xxx.x	xxx.x	xxx.x	xxx.x	xxx.x	xxx.x	xxx.x	xxx.x	xxx.x					
1365	xxx.x	xxx.x	xxx.x	xxx.x	xxx.x	xxx.x	xxx.x	xxx.x	xxx.x	xxx.x	xxx.x	xxx.x	xxx.x	xxx.x						
1360	xxx.x	xxx.x	xxx.x	xxx.x	xxx.x	xxx.x	xxx.x	xxx.x	xxx.x	xxx.x	xxx.x	xxx.x	xxx.x							
1355	xxx.x	xxx.x	xxx.x	xxx.x	xxx.x	xxx.x	xxx.x	xxx.x	xxx.x	xxx.x	xxx.x	xxx.x								
1350	xxx.x	xxx.x	xxx.x	xxx.x	xxx.x	xxx.x	xxx.x	xxx.x	xxx.x	xxx.x	xxx.x									
1345	xxx.x	xxx.x	xxx.x	xxx.x	xxx.x	xxx.x	xxx.x	xxx.x	xxx.x	xxx.x										
1340	xxx.x	xxx.x	xxx.x	xxx.x	xxx.x	xxx.x	xxx.x	xxx.x	xxx.x											
1335	xxx.x	xxx.x	xxx.x	xxx.x	xxx.x	xxx.x	xxx.x	xxx.x												
1330	xxx.x	xxx.x	xxx.x	xxx.x	xxx.x	xxx.x	xxx.x													
1325	xxx.x	xxx.x	xxx.x	xxx.x	xxx.x	xxx.x														
1320	xxx.x	xxx.x	xxx.x	xxx.x	xxx.x															
1315	xxx.x	xxx.x	xxx.x	xxx.x																
1310	xxx.x	xxx.x	xxx.x																	
1305	xxx.x	xxx.x																		
1300	xxx.x																			

Table 1. (cont'd) Certified value of mean DGD (fs) for SRM 2538 serial number ___ averaged over the wavelength range from “start wavelength” to “stop wavelength”. **Expanded uncertainty (95 % confidence interval) for any value in this table is x.x fs.**

stop wavelength (nm) ↓ \ start wavelength (nm) →	1350	1355	1360	1365	1370	1375	1380	1385	1390	1395	1400	1405	1410	1415	1420	1425	1430	1435	1440	1445
1550	xxx.x	xxx.x	xxx.x	xxx.x	xxx.x	xxx.x	xxx.x	xxx.x	xxx.x	xxx.x	xxx.x	xxx.x	xxx.x	xxx.x	xxx.x	xxx.x	xxx.x	xxx.x	xxx.x	xxx.x
1645	xxx.x	xxx.x	xxx.x	xxx.x	xxx.x	xxx.x	xxx.x	xxx.x	xxx.x	xxx.x	xxx.x	xxx.x	xxx.x	xxx.x	xxx.x	xxx.x	xxx.x	xxx.x	xxx.x	xxx.x
1640	xxx.x	xxx.x	xxx.x	xxx.x	xxx.x	xxx.x	xxx.x	xxx.x	xxx.x	xxx.x	xxx.x	xxx.x	xxx.x	xxx.x	xxx.x	xxx.x	xxx.x	xxx.x	xxx.x	xxx.x
1535	xxx.x	xxx.x	xxx.x	xxx.x	xxx.x	xxx.x	xxx.x	xxx.x	xxx.x	xxx.x	xxx.x	xxx.x	xxx.x	xxx.x	xxx.x	xxx.x	xxx.x	xxx.x	xxx.x	xxx.x
1630	xxx.x	xxx.x	xxx.x	xxx.x	xxx.x	xxx.x	xxx.x	xxx.x	xxx.x	xxx.x	xxx.x	xxx.x	xxx.x	xxx.x	xxx.x	xxx.x	xxx.x	xxx.x	xxx.x	xxx.x
1525	xxx.x	xxx.x	xxx.x	xxx.x	xxx.x	xxx.x	xxx.x	xxx.x	xxx.x	xxx.x	xxx.x	xxx.x	xxx.x	xxx.x	xxx.x	xxx.x	xxx.x	xxx.x	xxx.x	xxx.x
1520	xxx.x	xxx.x	xxx.x	xxx.x	xxx.x	xxx.x	xxx.x	xxx.x	xxx.x	xxx.x	xxx.x	xxx.x	xxx.x	xxx.x	xxx.x	xxx.x	xxx.x	xxx.x	xxx.x	xxx.x
1515	xxx.x	xxx.x	xxx.x	xxx.x	xxx.x	xxx.x	xxx.x	xxx.x	xxx.x	xxx.x	xxx.x	xxx.x	xxx.x	xxx.x	xxx.x	xxx.x	xxx.x	xxx.x	xxx.x	xxx.x
1510	xxx.x	xxx.x	xxx.x	xxx.x	xxx.x	xxx.x	xxx.x	xxx.x	xxx.x	xxx.x	xxx.x	xxx.x	xxx.x	xxx.x	xxx.x	xxx.x	xxx.x	xxx.x	xxx.x	xxx.x
1505	xxx.x	xxx.x	xxx.x	xxx.x	xxx.x	xxx.x	xxx.x	xxx.x	xxx.x	xxx.x	xxx.x	xxx.x	xxx.x	xxx.x	xxx.x	xxx.x	xxx.x	xxx.x	xxx.x	xxx.x
1500	xxx.x	xxx.x	xxx.x	xxx.x	xxx.x	xxx.x	xxx.x	xxx.x	xxx.x	xxx.x	xxx.x	xxx.x	xxx.x	xxx.x	xxx.x	xxx.x	xxx.x	xxx.x	xxx.x	xxx.x
1595	xxx.x	xxx.x	xxx.x	xxx.x	xxx.x	xxx.x	xxx.x	xxx.x	xxx.x	xxx.x	xxx.x	xxx.x	xxx.x	xxx.x	xxx.x	xxx.x	xxx.x	xxx.x	xxx.x	xxx.x
1590	xxx.x	xxx.x	xxx.x	xxx.x	xxx.x	xxx.x	xxx.x	xxx.x	xxx.x	xxx.x	xxx.x	xxx.x	xxx.x	xxx.x	xxx.x	xxx.x	xxx.x	xxx.x	xxx.x	xxx.x
1585	xxx.x	xxx.x	xxx.x	xxx.x	xxx.x	xxx.x	xxx.x	xxx.x	xxx.x	xxx.x	xxx.x	xxx.x	xxx.x	xxx.x	xxx.x	xxx.x	xxx.x	xxx.x	xxx.x	xxx.x
1580	xxx.x	xxx.x	xxx.x	xxx.x	xxx.x	xxx.x	xxx.x	xxx.x	xxx.x	xxx.x	xxx.x	xxx.x	xxx.x	xxx.x	xxx.x	xxx.x	xxx.x	xxx.x	xxx.x	xxx.x
1575	xxx.x	xxx.x	xxx.x	xxx.x	xxx.x	xxx.x	xxx.x	xxx.x	xxx.x	xxx.x	xxx.x	xxx.x	xxx.x	xxx.x	xxx.x	xxx.x	xxx.x	xxx.x	xxx.x	xxx.x
1570	xxx.x	xxx.x	xxx.x	xxx.x	xxx.x	xxx.x	xxx.x	xxx.x	xxx.x	xxx.x	xxx.x	xxx.x	xxx.x	xxx.x	xxx.x	xxx.x	xxx.x	xxx.x	xxx.x	xxx.x
1555	xxx.x	xxx.x	xxx.x	xxx.x	xxx.x	xxx.x	xxx.x	xxx.x	xxx.x	xxx.x	xxx.x	xxx.x	xxx.x	xxx.x	xxx.x	xxx.x	xxx.x	xxx.x	xxx.x	xxx.x
1550	xxx.x	xxx.x	xxx.x	xxx.x	xxx.x	xxx.x	xxx.x	xxx.x	xxx.x	xxx.x	xxx.x	xxx.x	xxx.x	xxx.x	xxx.x	xxx.x	xxx.x	xxx.x	xxx.x	xxx.x
1555	xxx.x	xxx.x	xxx.x	xxx.x	xxx.x	xxx.x	xxx.x	xxx.x	xxx.x	xxx.x	xxx.x	xxx.x	xxx.x	xxx.x	xxx.x	xxx.x	xxx.x	xxx.x	xxx.x	xxx.x
1550	xxx.x	xxx.x	xxx.x	xxx.x	xxx.x	xxx.x	xxx.x	xxx.x	xxx.x	xxx.x	xxx.x	xxx.x	xxx.x	xxx.x	xxx.x	xxx.x	xxx.x	xxx.x	xxx.x	xxx.x
1545	xxx.x	xxx.x	xxx.x	xxx.x	xxx.x	xxx.x	xxx.x	xxx.x	xxx.x	xxx.x	xxx.x	xxx.x	xxx.x	xxx.x	xxx.x	xxx.x	xxx.x	xxx.x	xxx.x	xxx.x
1540	xxx.x	xxx.x	xxx.x	xxx.x	xxx.x	xxx.x	xxx.x	xxx.x	xxx.x	xxx.x	xxx.x	xxx.x	xxx.x	xxx.x	xxx.x	xxx.x	xxx.x	xxx.x	xxx.x	xxx.x
1535	xxx.x	xxx.x	xxx.x	xxx.x	xxx.x	xxx.x	xxx.x	xxx.x	xxx.x	xxx.x	xxx.x	xxx.x	xxx.x	xxx.x	xxx.x	xxx.x	xxx.x	xxx.x	xxx.x	xxx.x
1530	xxx.x	xxx.x	xxx.x	xxx.x	xxx.x	xxx.x	xxx.x	xxx.x	xxx.x	xxx.x	xxx.x	xxx.x	xxx.x	xxx.x	xxx.x	xxx.x	xxx.x	xxx.x	xxx.x	xxx.x
1525	xxx.x	xxx.x	xxx.x	xxx.x	xxx.x	xxx.x	xxx.x	xxx.x	xxx.x	xxx.x	xxx.x	xxx.x	xxx.x	xxx.x	xxx.x	xxx.x	xxx.x	xxx.x	xxx.x	xxx.x
1520	xxx.x	xxx.x	xxx.x	xxx.x	xxx.x	xxx.x	xxx.x	xxx.x	xxx.x	xxx.x	xxx.x	xxx.x	xxx.x	xxx.x	xxx.x	xxx.x	xxx.x	xxx.x	xxx.x	xxx.x
1515	xxx.x	xxx.x	xxx.x	xxx.x	xxx.x	xxx.x	xxx.x	xxx.x	xxx.x	xxx.x	xxx.x	xxx.x	xxx.x	xxx.x	xxx.x	xxx.x	xxx.x	xxx.x	xxx.x	xxx.x
1510	xxx.x	xxx.x	xxx.x	xxx.x	xxx.x	xxx.x	xxx.x	xxx.x	xxx.x	xxx.x	xxx.x	xxx.x	xxx.x	xxx.x	xxx.x	xxx.x	xxx.x	xxx.x	xxx.x	xxx.x
1505	xxx.x	xxx.x	xxx.x	xxx.x	xxx.x	xxx.x	xxx.x	xxx.x	xxx.x	xxx.x	xxx.x	xxx.x	xxx.x	xxx.x	xxx.x	xxx.x	xxx.x	xxx.x	xxx.x	xxx.x
1500	xxx.x	xxx.x	xxx.x	xxx.x	xxx.x	xxx.x	xxx.x	xxx.x	xxx.x	xxx.x	xxx.x	xxx.x	xxx.x	xxx.x	xxx.x	xxx.x	xxx.x	xxx.x	xxx.x	xxx.x
1495	xxx.x	xxx.x	xxx.x	xxx.x	xxx.x	xxx.x	xxx.x	xxx.x	xxx.x	xxx.x	xxx.x	xxx.x	xxx.x	xxx.x	xxx.x	xxx.x	xxx.x	xxx.x	xxx.x	xxx.x
1490	xxx.x	xxx.x	xxx.x	xxx.x	xxx.x	xxx.x	xxx.x	xxx.x	xxx.x	xxx.x	xxx.x	xxx.x	xxx.x	xxx.x	xxx.x	xxx.x	xxx.x	xxx.x	xxx.x	
1485	xxx.x	xxx.x	xxx.x	xxx.x	xxx.x	xxx.x	xxx.x	xxx.x	xxx.x	xxx.x	xxx.x	xxx.x	xxx.x	xxx.x	xxx.x	xxx.x	xxx.x	xxx.x		
1480	xxx.x	xxx.x	xxx.x	xxx.x	xxx.x	xxx.x	xxx.x	xxx.x	xxx.x	xxx.x	xxx.x	xxx.x	xxx.x	xxx.x	xxx.x	xxx.x	xxx.x			
1475	xxx.x	xxx.x	xxx.x	xxx.x	xxx.x	xxx.x	xxx.x	xxx.x	xxx.x	xxx.x	xxx.x	xxx.x	xxx.x	xxx.x	xxx.x	xxx.x				
1470	xxx.x	xxx.x	xxx.x	xxx.x	xxx.x	xxx.x	xxx.x	xxx.x	xxx.x	xxx.x	xxx.x	xxx.x	xxx.x	xxx.x	xxx.x					
1465	xxx.x	xxx.x	xxx.x	xxx.x	xxx.x	xxx.x	xxx.x	xxx.x	xxx.x	xxx.x	xxx.x	xxx.x	xxx.x	xxx.x						
1450	xxx.x	xxx.x	xxx.x	xxx.x	xxx.x	xxx.x	xxx.x	xxx.x	xxx.x	xxx.x	xxx.x	xxx.x	xxx.x							
1455	xxx.x	xxx.x	xxx.x	xxx.x	xxx.x	xxx.x	xxx.x	xxx.x	xxx.x	xxx.x	xxx.x	xxx.x								
1450	xxx.x	xxx.x	xxx.x	xxx.x	xxx.x	xxx.x	xxx.x	xxx.x	xxx.x	xxx.x	xxx.x									
1445	xxx.x	xxx.x	xxx.x	xxx.x	xxx.x	xxx.x	xxx.x	xxx.x	xxx.x	xxx.x										
1440	xxx.x	xxx.x	xxx.x	xxx.x	xxx.x	xxx.x	xxx.x	xxx.x	xxx.x											
1435	xxx.x	xxx.x	xxx.x	xxx.x	xxx.x	xxx.x	xxx.x	xxx.x												
1430	xxx.x	xxx.x	xxx.x	xxx.x	xxx.x	xxx.x	xxx.x													
1425	xxx.x	xxx.x	xxx.x	xxx.x	xxx.x	xxx.x														
1420	xxx.x	xxx.x	xxx.x	xxx.x	xxx.x															
1415	xxx.x	xxx.x	xxx.x	xxx.x																
1410	xxx.x	xxx.x	xxx.x																	
1405	xxx.x	xxx.x																		
1400	xxx.x																			

Table 1. (cont'd) Certified value of mean DGD (fs) for SRM 2538 serial number ___ averaged over the wavelength range from "start wavelength" to "stop wavelength". **Expanded uncertainty (95 % confidence interval) for any value in this table is x.x fs.**

stop wavelength (nm) ↓ / start wavelength (nm) →	1450	1455	1460	1465	1470	1475	1480	1485	1490	1495	1500	1505	1510	1515	1520	1525	1530	1535	1540	1545
1650	xxx.x	xxx.x	xxx.x	xxx.x	xxx.x	xxx.x	xxx.x	xxx.x	xxx.x	xxx.x	xxx.x	xxx.x	xxx.x	xxx.x	xxx.x	xxx.x	xxx.x	xxx.x	xxx.x	xxx.x
1645	xxx.x	xxx.x	xxx.x	xxx.x	xxx.x	xxx.x	xxx.x	xxx.x	xxx.x	xxx.x	xxx.x	xxx.x	xxx.x	xxx.x	xxx.x	xxx.x	xxx.x	xxx.x	xxx.x	xxx.x
1640	xxx.x	xxx.x	xxx.x	xxx.x	xxx.x	xxx.x	xxx.x	xxx.x	xxx.x	xxx.x	xxx.x	xxx.x	xxx.x	xxx.x	xxx.x	xxx.x	xxx.x	xxx.x	xxx.x	xxx.x
1635	xxx.x	xxx.x	xxx.x	xxx.x	xxx.x	xxx.x	xxx.x	xxx.x	xxx.x	xxx.x	xxx.x	xxx.x	xxx.x	xxx.x	xxx.x	xxx.x	xxx.x	xxx.x	xxx.x	xxx.x
1630	xxx.x	xxx.x	xxx.x	xxx.x	xxx.x	xxx.x	xxx.x	xxx.x	xxx.x	xxx.x	xxx.x	xxx.x	xxx.x	xxx.x	xxx.x	xxx.x	xxx.x	xxx.x	xxx.x	xxx.x
1625	xxx.x	xxx.x	xxx.x	xxx.x	xxx.x	xxx.x	xxx.x	xxx.x	xxx.x	xxx.x	xxx.x	xxx.x	xxx.x	xxx.x	xxx.x	xxx.x	xxx.x	xxx.x	xxx.x	xxx.x
1620	xxx.x	xxx.x	xxx.x	xxx.x	xxx.x	xxx.x	xxx.x	xxx.x	xxx.x	xxx.x	xxx.x	xxx.x	xxx.x	xxx.x	xxx.x	xxx.x	xxx.x	xxx.x	xxx.x	xxx.x
1615	xxx.x	xxx.x	xxx.x	xxx.x	xxx.x	xxx.x	xxx.x	xxx.x	xxx.x	xxx.x	xxx.x	xxx.x	xxx.x	xxx.x	xxx.x	xxx.x	xxx.x	xxx.x	xxx.x	xxx.x
1610	xxx.x	xxx.x	xxx.x	xxx.x	xxx.x	xxx.x	xxx.x	xxx.x	xxx.x	xxx.x	xxx.x	xxx.x	xxx.x	xxx.x	xxx.x	xxx.x	xxx.x	xxx.x	xxx.x	xxx.x
1605	xxx.x	xxx.x	xxx.x	xxx.x	xxx.x	xxx.x	xxx.x	xxx.x	xxx.x	xxx.x	xxx.x	xxx.x	xxx.x	xxx.x	xxx.x	xxx.x	xxx.x	xxx.x	xxx.x	xxx.x
1600	xxx.x	xxx.x	xxx.x	xxx.x	xxx.x	xxx.x	xxx.x	xxx.x	xxx.x	xxx.x	xxx.x	xxx.x	xxx.x	xxx.x	xxx.x	xxx.x	xxx.x	xxx.x	xxx.x	xxx.x
1595	xxx.x	xxx.x	xxx.x	xxx.x	xxx.x	xxx.x	xxx.x	xxx.x	xxx.x	xxx.x	xxx.x	xxx.x	xxx.x	xxx.x	xxx.x	xxx.x	xxx.x	xxx.x	xxx.x	xxx.x
1590	xxx.x	xxx.x	xxx.x	xxx.x	xxx.x	xxx.x	xxx.x	xxx.x	xxx.x	xxx.x	xxx.x	xxx.x	xxx.x	xxx.x	xxx.x	xxx.x	xxx.x	xxx.x	xxx.x	
1585	xxx.x	xxx.x	xxx.x	xxx.x	xxx.x	xxx.x	xxx.x	xxx.x	xxx.x	xxx.x	xxx.x	xxx.x	xxx.x	xxx.x	xxx.x	xxx.x	xxx.x	xxx.x		
1580	xxx.x	xxx.x	xxx.x	xxx.x	xxx.x	xxx.x	xxx.x	xxx.x	xxx.x	xxx.x	xxx.x	xxx.x	xxx.x	xxx.x	xxx.x	xxx.x	xxx.x			
1575	xxx.x	xxx.x	xxx.x	xxx.x	xxx.x	xxx.x	xxx.x	xxx.x	xxx.x	xxx.x	xxx.x	xxx.x	xxx.x	xxx.x	xxx.x	xxx.x				
1570	xxx.x	xxx.x	xxx.x	xxx.x	xxx.x	xxx.x	xxx.x	xxx.x	xxx.x	xxx.x	xxx.x	xxx.x	xxx.x	xxx.x	xxx.x					
1565	xxx.x	xxx.x	xxx.x	xxx.x	xxx.x	xxx.x	xxx.x	xxx.x	xxx.x	xxx.x	xxx.x	xxx.x	xxx.x	xxx.x						
1560	xxx.x	xxx.x	xxx.x	xxx.x	xxx.x	xxx.x	xxx.x	xxx.x	xxx.x	xxx.x	xxx.x	xxx.x	xxx.x							
1555	xxx.x	xxx.x	xxx.x	xxx.x	xxx.x	xxx.x	xxx.x	xxx.x	xxx.x	xxx.x	xxx.x	xxx.x								
1550	xxx.x	xxx.x	xxx.x	xxx.x	xxx.x	xxx.x	xxx.x	xxx.x	xxx.x	xxx.x	xxx.x									
1545	xxx.x	xxx.x	xxx.x	xxx.x	xxx.x	xxx.x	xxx.x	xxx.x	xxx.x	xxx.x										
1540	xxx.x	xxx.x	xxx.x	xxx.x	xxx.x	xxx.x	xxx.x	xxx.x	xxx.x											
1535	xxx.x	xxx.x	xxx.x	xxx.x	xxx.x	xxx.x	xxx.x	xxx.x												
1530	xxx.x	xxx.x	xxx.x	xxx.x	xxx.x	xxx.x	xxx.x													
1525	xxx.x	xxx.x	xxx.x	xxx.x	xxx.x	xxx.x														
1520	xxx.x	xxx.x	xxx.x	xxx.x	xxx.x															
1515	xxx.x	xxx.x	xxx.x	xxx.x																
1510	xxx.x	xxx.x	xxx.x																	
1505	xxx.x	xxx.x																		
1500	xxx.x																			

Table 1. (cont'd) Certified value of mean DGD (fs) for SRM 2538 serial number ___ averaged over the wavelength range from "start wavelength" to "stop wavelength". **Expanded uncertainty (95 % confidence interval) for any value in this table is x.x fs.**

stop wavelength (nm) ↓ / start wavelength (nm) →	1550	1555	1560	1565	1570	1575	1580	1585	1590	1595	1600
1650	xxx.x	xxx.x	xxx.x	xxx.x	xxx.x	xxx.x	xxx.x	xxx.x	xxx.x	xxx.x	xxx.x
1645	xxx.x	xxx.x	xxx.x	xxx.x	xxx.x	xxx.x	xxx.x	xxx.x	xxx.x	xxx.x	
1640	xxx.x	xxx.x	xxx.x	xxx.x	xxx.x	xxx.x	xxx.x	xxx.x	xxx.x		
1635	xxx.x	xxx.x	xxx.x	xxx.x	xxx.x	xxx.x	xxx.x	xxx.x			
1630	xxx.x	xxx.x	xxx.x	xxx.x	xxx.x	xxx.x	xxx.x				
1625	xxx.x	xxx.x	xxx.x	xxx.x	xxx.x	xxx.x					
1620	xxx.x	xxx.x	xxx.x	xxx.x	xxx.x						
1615	xxx.x	xxx.x	xxx.x	xxx.x							
1610	xxx.x	xxx.x	xxx.x								
1605	xxx.x	xxx.x									
1600	xxx.x										

Table 2 lists a "high-accuracy" value of mean DGD over the range of the JME measurement system.

Table 2. Certified Value of Mean DGD for SRM 2538 (Serial Number ____)
Over the "High-Accuracy" Wavelength Range

Wavelength (nm) ± 5 nm		Mean DGD (fs)	Expanded uncertainty (fs)*
Start	Stop		
1481	1568	XXX.X	X.X

* Expanded uncertainty (k=2) gives the half width of an approximate 95 % confidence interval.

Details on the certification procedures and the associated uncertainties are given in Reference [2]. The uncertainties associated with each certified value are reported as "Expanded uncertainty", meaning a coverage factor of 2 is used to give an approximate 95 % confidence interval [3].

MEASUREMENT CONDITIONS

Device Warm Up: Before measuring the SRM, the power should be turned on and the unit allowed to warm up for at least one hour. The internal temperature can be checked by measuring the voltage across the BNC style connector on the back panel of the device. The output voltage is proportional to the internal temperature in kelvins (10 mV/K). The voltage should read _____V ± 0.05 V. If the voltage reading is outside this range, or if the device has not been powered up for at least one hour, the mean DGD is not certified.

Wavelength Range: The certified values of mean DGD are valid for measurements where the DGD is averaged over the stated wavelength ranges. All wavelengths reported are vacuum wavelengths.

The start and stop wavelengths are defined as the wavelength locations associated with the first and last DGD measurements (with uniformly spaced samples in between). This could cause confusion. For example, in the case of JME measurements, to measure the DGD at a given wavelength point requires the measurement of the Jones matrix of the device under test at two wavelengths on either side of the target wavelength. For example, a JME measurement of the DGD at 1480.5 nm might come as the result of measurements of the Jones transfer matrices at say 1480 nm and 1481 nm. The wavelength start and stop values of Tables 1 and 2 refer to the wavelengths at which the DGD values were measured (not wavelengths at which the Jones matrix was measured). So, for this JME example, if this was the first measurement point, the start wavelength would be reported as 1480.5 nm.

For the values in Table 1, the minimum wavelength-averaging scan range must be at least 50 nm. This prevents incorrect measurements due to possible multiple reflections within the device.

Care should be taken that the PMD measurement actually measures the mean DGD and not a weighted mean, as discussed in Scope of Use section.

Lead Birefringence: Lead birefringence on the PMD measurement system can impose an uncertainty on the measurement. Our calibrations were performed with a short lead length (~80 cm total) on the JME measurement system, and the PMD of the leads was measured and added to the uncertainty statement of Tables 1 and 2. We also randomized the orientation of the system fiber leads in between measurements in order to average away as much of the lead birefringence as possible. We recommend that the user of this SRM do the same. Note that the most complete randomization of the leads must include orientations where the fibers do not always lie in a single plane. Take care in reorienting the fiber leads that significant bending, which increases the fiber birefringence, is not introduced. Bend birefringence goes as R^{-2}, where R is the bend radius of the fiber [4]. We recommend that any bends in the fiber leads be restricted to radii greater than 5 cm. Some fraction of the lead birefringence might not average to 0, due to an inability to completely randomize the lead orientation or due to fixed sources of extraneous PMD (such as in the fiber connectors). Therefore, we recommend using the shortest possible leads and employing orientational averaging of lead birefringence for the best measurement. A measurement of the lead birefringence in the absence of the SRM gives an estimate of the uncertainty that can be expected due to lead birefringence.

Multiple Reflections: Multiple reflections in the optical path can cause incorrect measurements of device DGD. The most probable cause of multiple reflections is poor connections. The bulkhead connectors on the SRM unit are the FC/APC type (2.15 mm "wide key"). The cleanliness of the connectors is important. Accumulation of dust or dirt in the bulkhead adapter or on the connector ferrule endface can cause multiple reflections across the specimen,

which will add a random (with wavelength and temperature) noise to the measurement. Other sources of reflection in the measurement system are equally important. If the reflections cannot be reduced, multiple measurements can be made at slightly different wavelength sampling points or temperatures in order to average out the effects of multiple reflections.

REFERENCES

[1] Williams, P.A.; *Rotating Waveplate Stokes Polarimeter for Differential Group Delay Measurements of Polarization-Mode Dispersion, Applied Optics*; **38**, pp. 6508-6515 (1999).

[2] Williams, P.A.; Etzel, S.M.; Kofler, J.D.; Wang, C.M.; *Standard Reference Material 2538 for Polarization-Mode Dispersion (Non-Mode-Coupled)*; NIST Special Publication 260-145 (2002).

[3] Taylor, B.N.; Kuyatt, C.E.; Eds.; *Guidelines for Evaluating and Expressing the Uncertainty of NIST Measurement Results*; NIST Tech. Note 1297 (1994).

[4] Jeunhomme, Luc B.; *Single-Mode Fiber Optics: Principles and Applications*; (Mercel Dekker, Inc., New York, p. 74 (1990).

Users of this SRM should ensure that the certificate in their possession is current. This can be accomplished by contacting the SRM Program at: telephone (301) 975-6776; fax (301) 926-4751; e-mail srminfo@nist.gov; or via the internet http://www.nist.gov/srm.

Appendix B. Fixed Analyzer Measurements and Uncertainty

B.1 Fixed Analyzer Measurement Description

As mentioned, part of the certification of mean DGD is performed outside the actual wavelength measurement range of the JME technique. This is done based on published data of the birefringence of quartz and is a reliable technique. However, to be conservative, we verify the extrapolated mean DGD values by measuring them directly with a second technique - the Fixed Analyzer (FA) technique [6]. In this technique, the spectral transmission through the device under test (with a polarizer at the input and output of the device) gives a sinusoidal spectrum for non-mode-coupled PMD. The spectral density of peaks and valleys (extrema) is proportional to the mean DGD of the device over the wavelength range of measurement. In our implementation, an optical spectrum analyzer (OSA) detects the light from a spectrally broad light source (four edge-emitting light-emitting diodes coupled together to span a wavelength range from approximately 1200 nm to 1700 nm) as it is transmitted through a polarizer (computer-controllable orientation), the artifact, and an analyzer (Fig. B1). The spectral transmittance $I_{0°}$ is measured, then the input polarizer is rotated by 90° and the spectrum remeasured to yield $I_{90°}$. The relative orientation of the polarizer and analyzer with respect to each other is not critical and the 0° and 90° subscripts denote the angular change in the input polarizer and not necessarily its orientation relative to the output polarizer. The normalized transmission spectrum (difference over sum)

Figure B1. Schematic of Fixed Analyzer measurement; EELED is edge-emitting light-emitting diode, OSA is optical spectrum analyzer.

$$I_{\Delta/\Sigma}(\lambda) = \frac{I_{0^\circ}(\lambda) - I_{90^\circ}(\lambda)}{I_{0^\circ}(\lambda) + I_{90^\circ}(\lambda)}, \qquad \text{(B1)}$$

removes the source spectrum. The spectral density of extrema (peaks and valleys) in the normalized transmission spectrum is proportional to the mean DGD over the measured wavelength range [6]. Extrema were isolated using a thresholding algorithm [12] with a 0.15 thresholding level (i.e., peaks and valley were counted only when their height or depth was at least 15 % of the maximum extent of the data). The wavelength positions of extrema were estimated by performing a second-order polynomial least-squares curve fit to $I_{\Delta/\Sigma}(\lambda)$ in the region of each extremum. The mean DGD was estimated as [6]

$$\langle \Delta\tau \rangle_{\lambda_1-\lambda_2} = \frac{(N_e - 1)\lambda_F \lambda_L}{2(\lambda_F - \lambda_L)c}, \qquad \text{(B2)}$$

where N_e is the number of extrema, λ_F and λ_L are the locations of the first and last extrema, respectively, and c is the speed of light in vacuum.

FA measurements were made over three different wavelength spans in order to optimize the temporal resolution of mean DGD. The first scan was over the range from 1250 nm to 1650 nm. This scan was sampled with 581 points and a 0.1 nm spectral resolution setting. From this range, extrema were counted and the mean DGD over the range estimated from the wavelengths of the

minimum and maximum extrema (λ_F and λ_L respectively). A more precise measurement was made by making two more scans. These scans were made over the first and last 50 nm of the full scan range, with 581 sampled points and 0.1 nm spectral resolution. These "high resolution" scans enabled better location of the wavelengths of the minimum and maximum extrema λ_F and λ_L, respectively. Mean DGD could then be estimated from these three scans by using the 1250 nm to 1650 nm scan to provide the number of extrema N_e; the low-wavelength scan (1250 nm to 1300 nm) provided a high-resolution value for λ_F; and the high-wavelength scan (1600 nm to 1650 nm) provided a high-resolution value for λ_L. Then N_e, λ_F, and λ_L were used in Eq. (B2) to yield a high-resolution estimate of mean DGD over the nominally 1250 nm to 1650 nm wavelength range (the exact wavelength range is from λ_F to λ_L).

The two 50 nm scans can also be used independently to yield estimates of mean DGD centered at ~1275 nm and 1625 nm. These, plus the "high resolution" estimate centered at ~1450 nm give three estimates of mean DGD. The three mean DGD estimates from these scans were then compared to mean DGD estimates over the same wavelength ranges generated by extrapolating the results of our JME-based measurements, as mentioned above.

B.2 Fixed Analyzer Measurement Uncertainty

Since the FA measurements were used only to validate the estimated mean DGD values from JME measurements, it was not necessary to perform a full uncertainty analysis on the FA measurements. However, in order to increase our confidence in the measurements, we have identified and quantified the major sources of uncertainty in our FA measurements.

A Fixed-Analyzer measurement of mean DGD is a straightforward task when the device being tested is non-mode-coupled. Since the measurement consists of measuring the spectral density of extrema, the three necessary measurands are: identification of the positions of the peaks at the extremes of the wavelength range, measurements of that wavelength range, and the number of extrema in between.

False Peaks

Miscounting peaks is very unlikely since the spectral response is known to be sinusoidal for this non-mode-coupled artifact. Noise levels are not sufficient to generate a false extremum. To ensure this, extrema are counted only if they meet a fractional height criterion [12]. For this certification, a criterion of 0.15 was used (no feature was considered to be an extremum unless its height was greater than 15 % of the maximum vertical range of the spectral data). Since our system noise was well below 15 %, no measurement uncertainty is attributed to miscounting extrema.

Curve-Fitting Uncertainty

If the wavelengths of the extrema are not located accurately, an error can also arise. The peak (or valley) location is identified by fitting a second-order polynomial to the data around the peak (or valley). Error in this process could come from noise or distortion. The peak location error due to random noise on the sinusoidal spectrum can be estimated from the curve-fit itself. The curve-fitting was done through a least-squares method, and the covariance matrix was calculated from the normal equations and used to yield an uncertainty estimate due to amplitude noise on the data [10]. This value was measured to be typically less than 0.07 nm and so is a negligible

contribution to the uncertainty of the FA measurement. The possibility of amplitude distortion was also considered, but since this would affect the sinusoidal data symmetrically, it will not serve to shift the peak (or valley) location.

Relative Wavelength Accuracy of the Optical Spectrum Analyzer

Relative wavelength accuracy of the optical spectrum analyzer was measured using molecular gas absorption cells of hydrogen cyanide (HCN) and methane (CH_4) [13, 14]. Since the important quantity is the wavelength difference between the two measured extrema, the absolute wavelength accuracy of the optical spectrum analyzer is not important, but rather the linearity (the relative accuracy in measuring the separation of two wavelengths). To calibrate the wavelength linearity, light from an edge-emitting light-emitting diode (EELED) was transmitted through gas cells of HCN and CH_4 in series and the throughput spectrum detected on an optical spectrum analyzer (OSA). With the OSA centered at 1560 nm (50 nm span), the centers of three lines of the P branch, P(1), P(22), and P(24) of HCN were measured. The predicted center wavelengths of these lines are $\lambda_{P1} = 1543.1148$ nm; $\lambda_{P22} = 1559.814$ nm; and $\lambda_{P24} = 1561.6344$ nm [14]. Then, the OSA was centered at 1320 nm (50 nm span) and the center of the R(6) line of CH_4 was measured. The expected center wavelength of this line is $\lambda_{R6} = 1318.319$ nm [13]. The OSA was turned off and then back on and the measurement procedure repeated several times. The measurement was repeated again a day later.

The measurement procedure for this wavelength accuracy test is meant to simulate the procedure used in measuring the extremum locations in the SRM 2538 artifacts. To estimate the worst-case error in measuring the wavelength difference between extrema, we compiled the differences between the HCN lines and the CH_4 line for each scan. CH_4 and HCN wavelengths were compared only for data sets taken during the same scan set (i.e., absorption lines from HCN were not compared to the CH_4 line if the OSA was turned off between the measurements). The measured differences between the measured center wavelengths of the HCN P(1) and the CH_4 R(6) $\Delta\lambda_{P1R6,Meas}$, between HCN P(22) and CH_4 R(6) $\Delta\lambda_{P22R6,Meas}$, and between HCN P(24) and CH_4 R(6) $\Delta\lambda_{P24R6,Meas}$, are compared to the predicted (true) difference values $\Delta\lambda_{P1R6,True}$, $\Delta\lambda_{P22R6,True}$, and $\Delta\lambda_{P24R6,True}$. The discrepancy between measured and true difference values represents the wavelength errors for the wavelength range measured. Fig. B2 illustrates the wavelength errors measured. The worst-case disagreement was a 0.21 nm error between measured wavelength difference and true wavelength difference that came between the HCN P(22) and CH_4 R(6) lines.

Since typical measurements of the waveplate artifacts used extrema around 1250 nm and 1650 nm, the 1318 nm to 1560 nm differential wavelengths measured above were extrapolated to the 1250 nm to 1650 nm wavelength range. If we assume a linear relationship between relative wavelength error and absolute wavelength separation, the 0.21 nm worst-case error expands to $0.21\times(1650-1250)/(1560-1318) = 0.35$ nm. We take this to be the worst-case relative wavelength error experienced in our measurements of mean DGD using the FA measurement. Assuming a uniform distribution of error, this value is converted to a "standard uncertainty" by dividing by $\sqrt{3}$ [7]. We denote this value $U_\lambda = 0.20$ nm.

The uncertainty this produces in the mean DGD measurement can be quantified if we define $\Delta\lambda$ as the true wavelength separation between the extrema (at λ_F and λ_L) in the FA spectrum; then

the uncertainty in mean DGD due to this relative wavelength error will be given by the product $(U_\lambda / \Delta\lambda)\ \langle\Delta\tau\rangle$, which yields an uncertainty of $U_{\lambda,\mathrm{Broad}} = 0.15$ fs for a 300 fs artifact measured over a 400 nm range. For the mean DGD calculations performed only over the 50 nm ranges, this yields an uncertainty of $U_{\lambda,50} = 1.2$ fs for a 300 fs artifact.

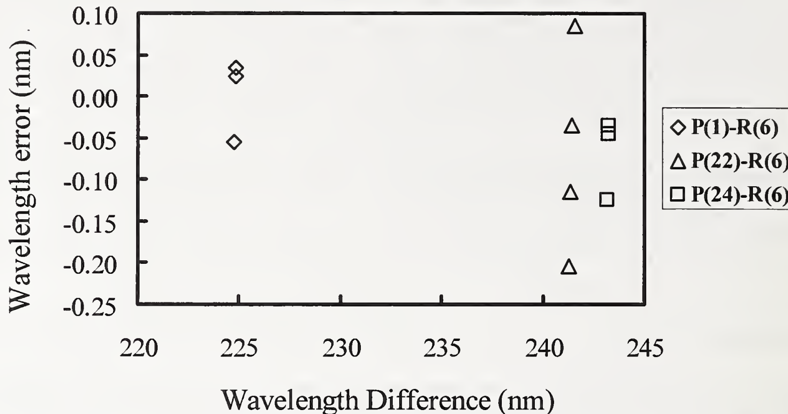

Figure B2. Relative wavelength errors of optical spectrum analyzer measurements. Y-axis is the error in wavelength difference between the two absorption lines measured, X-axis is the actual wavelength difference.

Peak Position Shift Due to Background Slope

Another difficulty that can come about in trying to locate an extremum is that a background slope to the spectrum can shift a peak to the "uphill" side of the slope or a valley to the "downhill" side. This is illustrated in Fig. B3. In order to estimate the uncertainty due to this effect, we quantify the shift as follows.

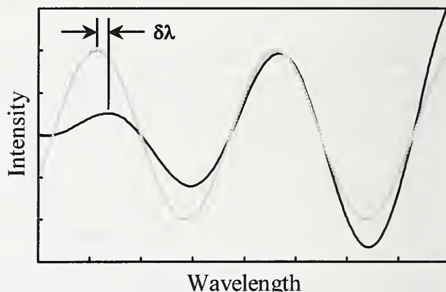

Figure B3. Illustration of shift of extremum wavelength when sinusoidal curve has a spectral slope (gray line is sinusoid, black line is sinusoid with slope).

Using the "difference-over-sum" intensity from the Fixed-Analyzer measurement (Eq. (B1)) gives a cosine response with wavelength

$$I_{\Delta/\Sigma} = \cos(2\pi\Delta n(\lambda)L/\lambda), \qquad \text{(B3)}$$

where Δn is the material (phase) birefringence and L is the length of this birefringent element. A slope to this response (due to lead

birefringence, or polarizer spectral dependence, etc.) would give the form

$$y = (a\lambda + b)\cos(2\pi\Delta n(\lambda)L/\lambda). \tag{B4}$$

An extremum occurs in the spectrum when the first derivative

$$\frac{dy}{d\lambda} = a\cos(\frac{2\pi\Delta nL}{\lambda}) - (a\lambda + b)\sin(\frac{2\pi\Delta nL}{\lambda})\left[\frac{2\pi\Delta nL}{-\lambda^2} + \frac{2\pi L}{\lambda}\frac{d\Delta n}{d\lambda}\right] \tag{B5}$$

vanishes. Setting Eq. (B5) to zero and substituting the differential group delay

$$\Delta\tau = \frac{\Delta n_g L}{c} = \left(\Delta n - \lambda\frac{d\Delta n}{d\lambda}\right)\frac{L}{c}, \tag{B6}$$

where Δn_g is the group birefringence, yields the transcendental equation for extremum wavelength

$$\frac{\eta\lambda_S{}^2}{2\pi\Delta\lambda\Delta\tau c} = -\tan(2\pi\Delta nL/\lambda_S), \tag{B7}$$

where $\Delta\lambda$ is the wavelength separation between two adjacent extrema and λ_S is the wavelength of one of these extrema. η is the normalized spectral slope

$$\eta = \frac{a\Delta\lambda}{a\lambda + b}. \tag{B8}$$

η is defined such that $\eta = 0.2$ would mean that the height of two adjacent peaks differ by 20 %. For small $\Delta\tau$ or large λ_S, Eq. (B2) can be approximated as

$$\Delta\lambda \approx \frac{\lambda_S{}^2}{2c\Delta\tau}, \tag{B9}$$

and Eq. (B7) becomes

$$\frac{\eta}{\pi} = -\tan(2\pi\Delta nL/\lambda_S). \tag{B10}$$

Restricting η to less than 0.5 will allow the small-angle approximation

$$\frac{\eta}{\pi} - p\pi \approx -2\pi\Delta nL/\lambda_S, \tag{B11}$$

or

$$\lambda_S \approx \frac{-2\pi\Delta nL}{\frac{\eta}{\pi} - p\pi}, \tag{B12}$$

where p is an integer, given by

$$p = \text{integer}\left[\frac{2\Delta nL}{\lambda_s}\right]. \qquad (\text{B13})$$

The shift in peak or valley wavelength as a function of slope comes from the difference between the extremum position λ_S having undergone the slope-induced shift, and the unshifted peak or extremum location λ_0 given by

$$\lambda_0 \approx \frac{2\pi\Delta nL}{p\pi}, \qquad (\text{B14})$$

so that

$$\delta\lambda = \lambda_S - \lambda_0 = \frac{2\Delta nL\eta}{p^2\pi^2 - \eta p} = \frac{1}{p^2\pi^2}\frac{2\Delta nL\eta}{(1-\eta/p\pi^2)}. \qquad (\text{B15})$$

To estimate $\delta\lambda$, we first calculate typical values of p. For an extremum at a wavelength of 1250 nm, and a mean DGD of 300 fs, $p = 144$; for an extremum at a wavelength of 1650 nm, $p = 109$. For $\eta<0.5$ and $p>109$, the large value of p makes the quantity in parentheses in Eq. (B15) approximately 1. Substituting Eq. (B13) into this large-p approximation of Eq. (B15) and approximating $\Delta\tau \approx \Delta nL/c$ ($\Delta n \approx \Delta n_g$) gives

$$\delta\lambda \approx \frac{\lambda_s^2\eta}{2\Delta\tau c\pi^2}. \qquad (\text{B16})$$

As an example, for λ_s=1650 nm and $\Delta\tau$ = 300 fs, the uncertainty due to a slope of η is given by $\delta\lambda \approx (1.5 \times 10^{-9}\text{m})\ \eta$. Using this estimate, we set a limit of $\eta \leq 0.2$ for our measurements–data sets are rejected if the measured FA spectrum shows extrema at the endpoints of the scan with $\eta>0.2$. This adds a wavelength uncertainty of up to 0.3 nm per extremum or a total uncertainty in wavelength span of 0.6 nm. Dividing by $\sqrt{3}$ (to get one standard uncertainty from the maximum value of a uniform distribution) [7] gives the uncertainty due to spectral slope $\delta\Delta\lambda_{\text{Slope}}$ = 0.3 nm. For a 300 fs artifact measured over an approximately 400 nm span, this uncertainty contributes U_{Slope} = (0.3 nm/400 nm) × 300 fs = 0.23 fs.

Lead Birefringence

The expected DGD error due to lead birefringence in our FA system is on the order of a few femtoseconds at most. However, due to the limit of the spectral width of our source, we cannot reliably measure mean DGD values lower than 10 to 20 fs. So we cannot directly measure the DGD error incurred due to lead birefringence by simply "shorting" the optical leads of the FA system and performing a mean DGD measurement. Instead, we estimate lead birefringence effects by measuring an artifact of known mean DGD. First, we estimate the systematic bias in DGD (that which does not go away by averaging multiple measurements with various lead reorientations). We do this by performing multiple measurements of mean DGD of the artifact with the system's fiber leads reoriented randomly between measurements. The average of these measurements is compared to the known mean DGD of the artifact. The difference in the measured mean and the true mean DGD will be considered to be the bias due to lead

birefringence. We used a reference fiber-pigtailed quartz plate whose mean DGD was accurately measured by other means [3] to be 445.5 fs (over the wavelength range of the FA measurement). We made eight FA measurements of mean DGD over the range of 1271 nm to 1639 nm. The average of the measured mean DGD values was 445.9 fs. This small discrepancy of 0.4 fs could easily be due to fiber lead birefringence. We assign an uncertainty due to the systematic bias due to lead birefringence $U_{lead} = 0.4$ fs.

Repeatability

Repeated FA measurements show some variation. This could be due to several factors, including lead birefringence. We estimate the uncertainty due to random errors by measuring the standard deviation of multiple measurements. Since we did not make sufficient FA measurements on any individual SRM 2538 artifact for a meaningful standard deviation estimate, we will instead use the standard deviation of multiple measurements on the 445.5 fs artifact described above. Eight FA measurements over the range 1271 nm to 1639 nm yielded a standard deviation of 0.81 fs.

Fixed Analyzer Uncertainty Summary

As discussed above, the FA measurements were done as a validation of the certifying JME measurements. So the uncertainty of the final values of the SRM 2538 artifacts do not contain elements due to the estimated uncertainty of the FA technique. Nevertheless, we calculate an estimate of the FA measurement uncertainty for completeness. The appreciable components of uncertainty found are given in Table B1. Adding the terms in quadrature gives the combined standard uncertainty, illustrating that the estimated uncertainty of the FA measurement is dominated by random uncertainty (likely due to birefringence of the fiber leads in the FA measurement system). The expanded uncertainty ("$k = 2$") for the FA measurement on a 300 fs device measured from approximately 1250 nm to 1650 nm is 1.9 fs.

Table B1. Summary of measurement uncertainty for the Fixed Analyzer technique on a 300 fs device.

Uncertainty Source	Standard Uncertainty (fs)
Relative wavelength error, $U_{\lambda,}$Wide	0.15
Spectral slope, U_{Slope}	0.23
Lead birefringence, U_{Lead}	0.4
Repeatability	0.81
Combined standard uncertainty, u_c	0.94
Expanded uncertainty, $U=2u_c$	**1.9**

Appendix C. Description of NIST Jones Matrix Eigenanalysis Polarimeter

Rotating-wave-plate Stokes polarimeter for differential group delay measurements of polarization-mode dispersion

Paul A. Williams

We present a description and detailed uncertainty analysis of a polarization-mode dispersion (PMD) measurement system that uses the Jones matrix eigenanalysis measurement technique based on a rotating-wave-plate Stokes polarimeter. The uncertainty of the system is 3.2 fs (~95% confidence interval) and is due primarily to PMD in the fiber leads of the measurement system.

OCIS codes: 060.2270, 060.2300.

1. Introduction

We have assembled and tested a Jones matrix eigenanalysis (JME) measurement system for polarization-mode dispersion (PMD) measurements based on a rotating-wave-plate technique. This technique was used as the primary technique for calibrating a National Institute of Standards and Technology (NIST) Standard Reference Material (SRM 2518) for the generation of mode-coupled PMD.[1] Here, we calculate the uncertainty of the measurements.

2. Description of Apparatus

Our JME system is shown schematically in Fig. 1. Light from a tunable laser diode is coupled into a single-mode fiber and goes through a polarization controller and then through the specimen. The polarization state of the exiting light is measured with a Stokes polarimeter. The unusual aspect of our system, which differentiates it from other JME systems,[2–4] is that the Stokes polarimeter is based on a rotating-wave-plate design that uses a single detector (as opposed to four in other designs). Our design was chosen to minimize the possible errors in multiple-detector systems such as the gain mismatch that results from temperature gradients. Although multiple-detector implementations can calibrate out static gain mismatches between detectors and periodically recalibrate to minimize the effects of transitory gain mismatch due to thermal gradients, the single-detector design is simpler in that it does not require these calibrations. A personal computer is used to control the system and to analyze the intensity measurements.

The tunable laser has a range of 1480–1570 nm with a linewidth of less than 100 kHz. The free-space polarization controller consists of $\lambda/4$ and $\lambda/2$ wave plates, followed by a polarizer. The wave plates are used to manipulate the polarization state between the laser and the polarizer in order to optimize the power throughput. The polarizer P_1 has an extinction ratio of >40 dB from 1470 to 1570 nm. The orientations of the wave plates and the polarizer are computer controllable (the polarizer's orientational resolution is 0.18°).

The Stokes polarimeter consists of a graded-index lens that launches the light from the fiber onto a $\lambda/4$ waveplate (true zero-order polymer) spinning at 1450 rpm (~24 Hz). The light is then incident upon a Glan–Thompson analyzer P_2 whose extinction axis orientation is defined as horizontal. Exiting the analyzer, the light is incident on a lens and focused on an InGaAs photodiode. The output of the photodiode is read by a lock-in amplifier and a digital voltmeter (DVM). Measuring the dc, $2f$, and $4f$ components of this signal allows the calculation of the Stokes vector of the light (see Appendix A for details of the analysis).

The PMD of the test device is measured according to the technique of Heffner.[2] For a given test specimen, the Stokes vector of the transmitted light is measured at a particular wavelength for three dif-

P. A. Williams (paul.williams@nist.gov) is with the Optoelectronics Division, National Institute of Standards and Technology, MS 815.02, 325 Broadway, Boulder, Colorado 80303-3328.

Received 20 April 1999; revised manuscript received 12 July 1999.

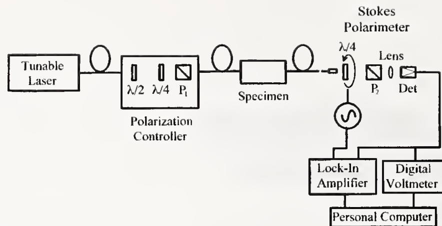

Fig. 1. Schematic of the rotating-wave-plate Stokes polarimeter for measuring DGD.

ferent launch polarization states (in our case, we use P_1 to generate three linear states at $\varphi + 0°$, $\varphi + 45°$, and $\varphi + 90°$ where φ is an arbitrary reference angle). From these three measured Stokes vectors, the Jones transfer matrix of the test specimen (including the fiber leads) is calculated at the test wavelength. Then, the wavelength is changed and the process repeated giving a second Jones matrix at the new wavelength. Again following Heffner, we calculate the differential group delay (DGD; or $\Delta\tau_g$) as

$$\Delta\tau_g = \left|\frac{\arg(\rho_1/\rho_2)}{\Delta\omega}\right|, \tag{1}$$

where ρ_1 and ρ_2 are the eigenvalues of the matrix product

$$T(\omega + \Delta\omega)T^{-1}(\omega), \tag{2}$$

formed from the Jones transfer matrices $T(\omega)$ and $T(\omega + \Delta\omega)$ of the test device measured at the two optical frequencies ω and $\omega + \Delta\omega$.

Here a couple of clarifying notes are appropriate. A DGD measurement requires measurement of the Jones matrix of the test specimen at two different optical frequencies. We usually refer to this difference in terms of wavelength as the step size. If the Jones matrices were measured at λ_1 and λ_2, then the calculated DGD would be reported as the DGD at the average of those two wavelengths. For example, if a scan of DGD versus wavelength involved measuring the Jones matrices at 1500, 1502, 1504, and 1506 nm (a 2-nm step size), then it would yield DGD values at 1501, 1503, and 1505 nm. For clarity, we use the term DGD to refer to the instantaneous group delay between the two principal states of polarization at a given wavelength. The term PMD is used to refer to the mean of multiple DGD measurements over a given wavelength range.

3. Uncertainty Analysis

The purpose of developing this JME measurement system was to provide accurate measurements of a NIST SRM for characterizing mode-coupled PMD.[1] The SRM is a stack of ~35 quartz wave plates cemented together with random angular orientations and pigtailed with single-mode fiber. Uncertainties in the assembly of this device prevented us from calculating its theoretical PMD; therefore the calibration of this device depends solely on the calibration of the JME system used to do the measurement.

We estimated the measurement system's type A (statistical) (Ref. 5) uncertainties from the standard deviation of multiple measurements. We also compared this result with the quadrature sum of estimated type A error sources.

Type B (nonstatistical) (Ref. 5) uncertainties, however, cannot be directly measured with self-consistency arguments (standard deviation, etc.). To identify them, we used two approaches. First, we tested the system by measuring a single pigtailed quartz plate (non-mode-coupled) with a known PMD. Second, we estimated the systematic uncertainties from the known inaccuracies of the experimental equipment.

The algorithm that derives PMD from the measured intensities is a complicated expression that does not lend itself to error analysis through simple propagation of errors. The best way to estimate PMD measurement uncertainty is through computer simulation. We wrote a program to generate the wavelength-dependent Jones matrices that represent a non-mode-coupled PMD element measured in the presence of equipment inaccuracies (polarizer misalignment, improper wave-plate retardance, etc.). These Jones matrices were fed into the same algorithms used by our JME system to calculate the measured DGD, and then this value was compared with the true theoretical value. The discrepancy is the error due to the equipment inaccuracies. This simulated experiment was repeated multiple times with various fiber pigtail orientations and different theoretical DGD values. The difference between these simulated DGD values (measured and true) gives an expected uncertainty due to equipment inaccuracies. Our simulations were run with DGD values uniformly distributed from 0 to 1 ps—the expected measurement range of our JME system for measuring the SRM artifacts.

In summarizing the uncertainties due to equipment inaccuracies, we found that most resulting measurement errors are random and that the significant systematic ones are systematic only for fixed measurement conditions. That is, if multiple measurements are made with the input state of polarization varied between measurement runs, all significant error sources will be random with a mean error of zero. We accomplished this by changing the launch polarizer offset (φ as mentioned above) before each DGD-versus-wavelength run. We also varied the launch polarization state by changing the orientation of the fiber leads connecting the specimen. Six possible sources of random error due to equipment inaccuracies were identified and are described below.

A. Random Uncertainties

1. *Polarizer Misalignment*

We measured the Jones matrix of the test device by launching three states of polarization with relative orientations of 0°, 45°, and 90°. Alignment errors of the polarizers cause negligible uncertainty in the measured DGD. As stated before, the 0°, 45°, and 90° angles are only relative orientations with respect to some arbitrary alignment. That means polarizer orientations of 10°, 55°, and 100° would give identical DGD values. It is only the relative offset between polarizer orientations that might cause trouble (0°, 46°, and 90° for example). We found from simulation that polarizer misalignments as large as ±2° give worst-case DGD errors less than $\pm 6 \times 10^{-4}$ fs. Since our expected alignment errors are on the order of 0.18°, polarizer misalignment is a negligible error source.

2. *Lock-in Amplifier Phase Errors*

Appendix A shows that the phase setting of the lock-in amplifier can be important. The signal distribution between the sine and the cosine components at $4f$ is determined by the phase setting of the lock-in amplifier. Phase errors at $4f$ cause leakage between S_1 and S_2 (horizontal and 45° linear states). This corresponds to a rotation of the defined Poincaré sphere about its polar axis. This leakage has no effect on DGD measurements, where the important parameter is the relative travel of the polarization state on the Poincaré sphere as a function of wavelength. However, incorrectly identifying S_1 and S_2 (C and D in Appendix A) does affect our measurement of degree of polarization (DOP). DOP is calculated as

$$\mathrm{DOP} = \frac{S_0 - (S_1^2 + S_2^2 + S_3^2)^{1/2}}{S_0}. \tag{3}$$

Since C and D are not used symmetrically in the Stokes parameter definitions of Eqs. (A6), phase errors at $4f$ cause us to misreport the DOP. This is important because we use DOP measurements to ensure that the system is well behaved during the measurement (we know that the DOP should be close to 1.0 and be a constant independent of measurement parameters). We easily set the $4f$ phase by launching a linear polarization state into the Stokes polarimeter (a bulk polarizer is placed immediately in front of the rotating wave plate at 90° with respect to the analyzer P_1 in Fig. 1). This vertical linear state has only a negative C component and no D component. We set the phase at $4f$ on the lock-in accordingly.

However, the phase setting at $2f$ directly affects the measured DGD, but fortunately by a small amount and in a random way. Since there is no $2f$ cosine term in Eqs. (A2)–(A5), errors in setting the phase at $2f$ reduce the amplitude of B. This distorts the Poincaré sphere by flattening it at the poles and can result in a second-order error in measurement of arc length on the sphere. We set the phase at $2f$ by launching a nearly circular state into the Stokes polarimeter and then adjusting the phase to optimize the amplitude of the B component. Our repeatability in setting phase is always less than 1°. So, we simulated the error in PMD measurements resulting from 1° phase errors on both $2f$ and $4f$ measurements and found the standard deviation to be 0.06 fs (for $\Delta\omega$ step sizes—see Eq. (2)—corresponding to 3 nm). Thus phase errors represent a negligible contribution to the measurement uncertainty.

3. *Stokes Polarimeter*

The primary source of errors in the measurement of the Stokes vector comes from imperfections in the quarter-wave retarder. The derivation of Appendix A assumes the retarder to be exactly quarter wave. If it is not, the result will be errors in the measured Stokes parameters. These errors are correctable if the true retardance of the wave plate is known. For a non-quarter-wave retarder, the true Stokes parameters are given by

$$\begin{aligned} S_0 &= A - C/\tan^2(\delta/2), \\ S_1 &= 2C/2\sin^2(\delta/2), \\ S_2 &= 2D/2\sin^2(\delta/2), \\ S_3 &= B/\sin(\delta), \end{aligned} \tag{4}$$

where δ is the true retardance of the nominally quarter-wave plate. These equations reduce to Eqs. (A6) when δ = 90°. So, if the actual retardance of the quarter-wave plate is known, the true Stokes parameters can still be obtained. A problem occurs when there are unknown retardance variations in the quarter-wave plate.

The retardance of the wave plate is specified within 1.2° (manufacturer's specification of spatial uniformity). Computer simulations show that a 1.2° retardance error yields random measurement errors with a standard deviation of 8 fs. Other errors in retardance can result from a tilt between the wave plate and the incident beam and the wavelength dependence of the retardance. We measured the wavelength dependence of the quarter wave-plate retardance using the NIST rotating-polarizer polarimeter.[6] This wavelength dependence is used with Eqs. (4) for automatic correction of the wavelength-dependent retardance errors during the measurement.

Another potential source of uncertainty comes when the wave plate is tilted off axis. Wave-plate tilt takes two forms: Wobble is tilt of the wave plate in its mount with respect to the rotation axis, and axis tilt is tilt of the mount (rotation axis) with respect to the beam (Fig. 2). Pure wobble causes the light to enter the wave plate at nonnormal incidence, but with a constant angle of incidence with respect to the fast and the slow axes of the plate during rotation. This results in a systematic bias to the effective retardance of the wave plate. On our setup, we measured the wobble to be less than 0.4°. This translates to an internal (to the wave plate) incidence

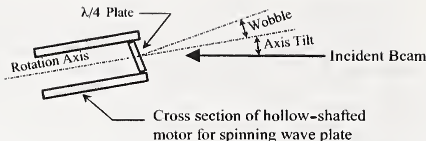

Fig. 2. Two possible types of wave-plate angular misalignment.

angle of 0.26°. This nonnormal incidence causes a systematic error in the wave-plate retardance of ±0.001°.[7] This is orders of magnitude below the uncertainty owing to wave-plate uniformity and is considered negligible. The effects of axis tilt are more difficult to quantify. The source of errors is still the same as with wobble—nonnormal incidence alters the effective retardance of the wave plate. However, as the plate rotates, the effective retardance changes, depending on whether the tilt is toward the fast or the slow axis (or somewhere between). We did not derive a closed-form expression to quantify this error, which depends on the DGD of the device being measured. Instead, we used computer simulation to predict the possible range of errors resulting from axis tilt. We measured the axis tilt to be $<0.4°$ (external angle). Our simulation used a conservative estimate of 1° axis tilt, which gave a random error with a worst-case value of <0.03 fs. This represents a negligible error source.

4. Laser Wavelength

A significant source of uncertainty in the experiment can be attributed to uncertainty in laser wavelength. Using a wavemeter, we calibrated the wavelength error of the tunable laser (agreement between the target wavelength and the actual wavelength). Since we did not have a wavemeter available for real-time monitoring of the actual laser wavelength, we treated the wavelength uncertainty as an error source. In the measurement of DGD, a critical parameter is the wavelength difference $\Delta\lambda$ between adjacent measurement points. This is because the instantaneous DGD is given as $|dS/d\omega|$, the change in Stokes vector for a given change in optical frequency. An error in $\Delta\lambda$ therefore produces a proportional error in DGD. This error increases as the wavelength step size decreases. Our tunable laser exhibited a wavelength uncertainty of ±0.008 nm (one standard deviation). At, say, 8-nm step sizes, this represents only a 0.1% error, but at 0.8-nm step sizes, it becomes a 1% error. Fortunately, this error can be reduced by averaging of data (or by real-time monitoring of the laser wavelength with a wavemeter).

Computer simulation supports these statements. We ran simulations using worst-case wavelength errors of three times the observed ±0.008-nm standard deviation. For wavelength steps of 1 nm, random PMD errors with standard deviation $\sigma = 12$ fs occurred, 2-nm step sizes yielded $\sigma = 5.7$ fs, and 3-nm steps gave $\sigma = 3.6$ fs, for a nominal DGD of 0.5 ps.

Table 1. Estimated Random Uncertainties

Error Source	Standard Uncertainty, fs
Wavelength uncertainty (3-nm step size)	3.6
Multiple reflections (0.2% per surface)	3.6
Retardance error in λ/4 plate	8
Combined Standard Uncertainty	9.5

5. Multiple Reflections

One error that could occur independent of deficiencies in the measurement apparatus comes from multiple reflections. If two reflections somewhere in the test system occur with one on each side of the test specimen, then the effect will be a cavity with the test device inside. This means that the measured PMD includes coherently added PMD contributions from the multiple paths of the device. This type of phenomenon has been discussed in depth with regard to measurements of optical retardation.[8] In the case of PMD, the critical parameters are the same. The higher the quality factor Q of the cavity created by the reflections, the larger the distortion of the measured PMD. However, the saving fact is that the multiple delays with each reflection add coherently and so are very sensitive to wavelength and cavity length. Thus in PMD measurements, the effects of multiple reflections may be averaged away by multiple measurements either at slightly different temperatures (fractions of 1 °C should be enough) or at wavelengths that are different by fractions of 1 nm. Computer simulation showed that a cavity with intensity reflections of 0.2% (−27 dB) at each end and a true DGD of 0.5 ps generates a random DGD measurement error with a standard deviation of 3.6 fs.

6. Polarization Extinction Ratio

The two polarizers used in the system have extinction ratios ≥40 dB. However, the extinction ratio of the polarizers is not critical since the JME measurement calculates the DGD only from the portion of light that is completely polarized. A poor extinction ratio of P_1 would reduce the degree of polarization through the test device, but only the polarized part of the light is used in the DGD measurement. Poor extinction by P_2 would underreport the DOP of the light going through the test device. But, low extinction ratios in either P_1 or P_2 do not directly affect the PMD accuracy. The only reason for high extinction ratios on the polarizers is to optimize the optical throughput for purposes of noise reduction.

7. Summary of Random Uncertainties

Table 1 lists the theoretical sources of random uncertainty (one standard deviation) and their combined standard uncertainty (quadrature addition) total of 9.5 fs. We directly measured the standard deviation of DGD measurements with a pigtailed quartz plate (0.4464 ps). We made 50 scans over the range 1480–1569 nm, giving a total of 1008 data points.

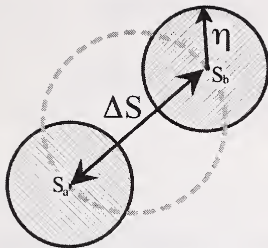

Fig. 3. Schematic illustration that the distance ΔS between two Stokes vectors ($\mathbf{S_a}$ and $\mathbf{S_b}$) is systematically biased by the presence of random Stokes noise (of amplitude η).

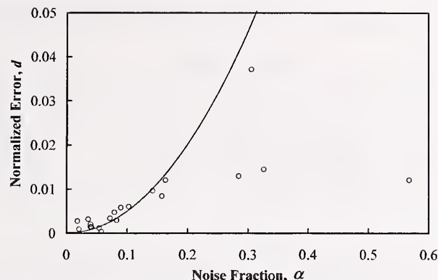

Fig. 4. Normalized systematic error $d(\alpha)$ versus noise fraction α. Solid curve is theoretical prediction from Eq. (5), and circles are data points from two different quartz plates sampled at different wavelength step sizes.

The measured sample standard deviation was 5.2 fs, and the standard deviation of the mean was 0.20 fs. This 5.2-fs experimental standard deviation is well within our 9.5-fs estimate.

B. Systematic Uncertainties

1. *Systematic Errors from Random Noise*

It is possible for a random-noise source to add a systematic bias to PMD measurements. This comes from the fact that DGD is a scalar quantity resulting from a vector measurement. The JME measurement of DGD is equivalent to measurement of the change in the output Stokes vector in response to a change in the optical frequency of the source $|\Delta S/\Delta\omega|$. Figure 3 shows the Stokes vectors ($\mathbf{S_a}$ and $\mathbf{S_b}$) measured at λ_a and λ_b, respectively. If the measured Stokes vectors are subject to some noise η, they will randomly describe a set of points within a circle of radius η whose center is the location of the noise-free Stokes vector. When measuring arc length on the sphere, the average of multiple JME system measurements really averages the distance between points randomly located within circle a and points randomly located within circle b. This operation does not average to the distance between the circles' centers ($\Delta S = |\mathbf{S_a} - \mathbf{S_b}|$) but rather to something greater than that. This seems counterintuitive, but consider the case in which ΔS approaches 0; measuring ΔS then amounts to the average distance between two points randomly chosen within a circle of radius η. Clearly, this average distance is greater than 0; thus we have a positive systematic bias. This normalized error in measuring DGD in the presence of noise can be approximated as

$$d(\alpha) = \frac{\int_0^{2\pi}\int_0^{2\pi} [(1+\alpha\cos\theta-\alpha\cos\varphi)^2+(1+\alpha\cos\theta-\alpha\cos\varphi)^2]^{1/2}\,d\theta d\varphi}{\int_0^{2\pi}\int_0^{2\pi} d\theta d\varphi}, \tag{5}$$

where the noise fraction $\alpha = \eta/\Delta S$. This normalized theoretical bias is plotted as a function of α in Fig. 4 (solid curve). The data points are experimental data from measurements of two quartz plates of PMD at 0.218 and 0.4464 ps. We varied α experimentally by sampling with various wavelength step sizes. As Fig. 4 shows, the systematic bias in the measurements agrees well with theory for small values of α. To determine α for the experimental data, we knew the target value of ΔS, and we used η as the free parameter. The points in Fig. 4 are scaled with $\eta = 0.015$. These values agree fairly well with the estimated η values for our apparatus. We can estimate η as $\eta_S + \eta_\lambda$, where η_S is a direct measurement of the random noise on the Stokes vector and η_λ is the estimated noise due to the random wavelength variations. The expression $\eta_S + \eta_\lambda$ yields a value between 0.006 and 0.009. This discrepancy between predicted and fitted values of η implies that there are still other random-noise sources that we have not accounted for.

This possible systematic error in measurements must be considered when the PMD-induced Stokes vector change is small with respect to the absolute noise on the measurement. In our calibration measurements, this was not a factor since our measurements were carried out with step sizes between 2.7 and 8 nm ($\alpha < 0.009$), which yields negligible systematic uncertainties. However, as can be seen from Fig. 4, the experimental data level off without reaching zero at the smallest values of α. This effect, which likely comes from some other source of error

Table 2. Summary of Measurement Uncertainty for JME Measurement System

Uncertainty Source	Method	Standard Uncertainty, fs
Experimental random errors	Measured standard deviation of the mean of repeated independent measurements	0.20
Systematic bias due to random noise	From random-noise estimates	1.0
Uncertainty of quartz artifact calibration	Theoretical calculation	1.2
Combined standard uncertainty	$u_c = [\Sigma u_i^2]^{1/2}$	1.6
Expanded uncertainty	$U = 2u_c$	3.2

than was considered here, can be taken into account by addition of a conservative +0.2% (~1 fs for our ~0.5-ps device) contribution to the uncertainty. Although these systematic errors are practically negligible for the current measurements, this bias mechanism must be kept in mind because it limits the minimum wavelength step that may be used in measurements. For example, given the noise of this system, a <0.25% systematic uncertainty requirement means that a 0.1-ps device must be measured with a step greater than 0.5 nm and that a 1-ps device requires steps greater than 0.2 nm.

2. *Comparison to Artifact*

To calibrate our JME measurement system and identify systematic errors, we measured our well-characterized pigtailed quartz plate (Appendix B). As described above, 1008 measurements were made over the wavelength range 1480–1569 nm with step sizes between 2.7 and 8 nm. The average of the measurements was 0.4465 ps with a sample standard deviation of 5.2 fs. The difference between our measurement of the PMD of the quartz plate and the 0.4464-ps theoretical value is 0.1 fs, well within the 1.2 fs uncertainty of the quartz plate's theoretical PMD.

3. *Quality of Data*

Since much of the uncertainty analysis of this system relies on assumptions about the uncertainties of the measurement equipment, it is useful to have an independent means of judging if the data has been taken under the assumed conditions. The measured DOP was used for this purpose. Particular error sources such as wave-plate retardance errors, lock-in phase errors, Stokes noise, and dc measurement errors cause the measured DOP to fluctuate around its true value. For these error sources, the size of DOP fluctuations can be an indication of the magnitude of the measurement uncertainty. We have found through simulation that for uncertainties within ranges that support our error-analysis assumptions, the DOP varies by as much as ±5% or so. So, to be conservative, we measure DOP simultaneously with DGD and use only those DGD values that fluctuate about the mean by less than 3%. Experimentally, we find a mean DOP of 0.97 for measurements with our system. So we throw out DGD values that have an associated DOP outside of the range 0.94 < DOP < 1.0. As a test, we compared mean DGD measurements made on the pigtailed quartz-plate artifact with and without this DOP criteria and found only a 0.01-fs difference. This supports our assumptions regarding equipment uncertainties and implies that this DOP criteria was not necessary.

4. Conclusions

Table 2 lists the significant uncertainties (in femtoseconds) that we have calculated for our measurement system for measurements on a ~0.5-ps device. Adding the three uncertainties in quadrature and multiplying by a coverage factor of 2 gives an expanded uncertainty of 3.2 fs. For comparison, we are aware of one other published uncertainty analysis for a polarization-state analyzer that uses the Stokes vector arc analysis technique for DGD measurement.[4]

Appendix A: Operation of Stokes Polarimeter

The polarization state of the light is determined with a rotating-wave-plate Stokes polarimeter.[9] As Fig. 1 shows, the Stokes polarimeter is simply a spinning quarter-wave plate in front of a fixed polarizer, followed by a detector. Using a phase-sensitive lock-in amplifier and a dc voltmeter allows the measurement of the dc, $2f$, and $4f$ (both in-phase and quadrature components). The four Stokes parameters can be found from these components. At the detector, the intensity as a function of wave-plate orientation θ and the Stokes parameters of the incident light is[9]

$$I(\theta) = \frac{1}{2}(S_0 + S_1 \cos^2 2\theta + S_2 \sin 2\theta \cos 2\theta + S_3 \sin 2\theta), \quad (A1)$$

where S_0 is the first Stokes parameter of the incident light, and so on. One can find the Stokes parameters by Fourier analyzing the transmitted intensity. The dc signal is measured, with a DVM, as

$$A = \frac{1}{\pi}\int_0^{2\pi} I(\theta)\mathrm{d}\theta, \quad (A2)$$

where $I(\theta)$ is the detected intensity when the wave plate has orientation θ. The $2f$ component is measured with the lock-in amplifier to give

$$B = \frac{2}{\pi}\int_0^{2\pi} I(\theta)\sin(2\theta)\mathrm{d}\theta. \quad (A3)$$

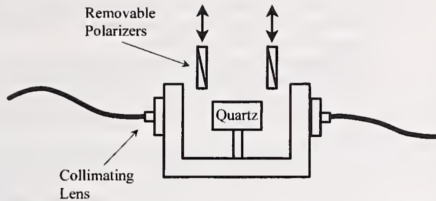

Fig. 5. Diagram of non-mode-coupled PMD test artifact. With removable polarizers that can be inserted to make a wavelength-scanning measurement independent of lead PMD.

The $4f$ components are

$$C = \frac{2}{\pi} \int_0^{2\pi} I(\theta)\cos(4\theta)\mathrm{d}\theta, \quad \text{(A4)}$$

$$D = \frac{2}{\pi} \int_0^{2\pi} I(\theta)\sin(4\theta)\mathrm{d}\theta. \quad \text{(A5)}$$

The Stokes parameters are found by combination of the measured values A, B, C, and D to give

$$\begin{aligned} S_0 &= A - C, \\ S_1 &= 2C, \\ S_2 &= 2D, \\ S_3 &= B. \end{aligned} \quad \text{(A6)}$$

The resulting Stokes vector is then used along with the two other Stokes vectors measured for different orientations of the input polarizer to calculate the Jones transfer matrix of the device under test. This procedure is also included in Heffner's letter.[2]

The advantage of the rotating-wave-plate method of measuring the Stokes parameters is that all four parameters are measured with the same detector. This eliminates the errors that can result from a four-detector system with mismatched gains.

The dc level A is measured with a DVM as opposed to the lock-in amplifier used for B, C, and D. This means that errors in the absolute calibration between the DVM and the lock-in could be important. However, the dc level is used only in the calculation of DOP and has no effect on measured DGD.

Appendix B: Quartz-Plate Reference Device

To assess the accuracy of the measurement system, we measured an artifact of known PMD and compared our measured result with the known value. We did this by assembling a non-mode-coupled artifact from a single quartz plate pigtailed with single-mode fiber (Fig. 5). We measured the thickness and wedge of the quartz plate accurately and combined that information with group birefringence data to calculate the expected DGD for propagation through the quartz plate. The uncertainty of the DGD of the plate comes from uncertainties of the thickness and index measurements, birefringence in the fiber pigtails, and multiple reflections off the endfaces of the quartz.

We measured the thickness of the quartz plate with a coordinate-measurement machine. The plate's thickness was 14.243 ± 0.002 mm (±0.014%), measured at 20.2 ± 0.2 °C. Another factor in the uncertainty is the effective thickness of the quartz plate. Although we accurately know the thickness of the plate, if the probe light enters the plate at a nonnormal incidence, the optical path length will be different. We measured the angle of incidence φ for He–Ne light at 632.8 nm to be 0.31°, which translates to an internal angle of 0.21°. Assuming this angle to be the same as for light at the actual wavelength of use (~1550 nm), we calculate the tilt-induced length error to be +0.0001 − 0 mm, or <0.0007%, again negligible in light of the absolute thickness uncertainty of ±0.014%.

We obtained the quartz birefringence in two different ways. First, comparison of the numbers from the literature[10–12] illustrates a discrepancy in the quoted values (>0.18%). So, as a second approach, we measured group birefringence ourselves. The quoted journals report phase birefringence as opposed to group birefringence. It is the group birefringence that determines the DGD. The relation between the two is[13]

$$\Delta n_g = \Delta n_p - \lambda \frac{\mathrm{d}(\Delta n_p)}{\mathrm{d}\lambda}. \quad \text{(B1)}$$

We made the group birefringence measurement by a wavelength scan of the quartz plate (Fig. 5). We inserted polarizers between the graded-index lenses of the fiber pigtails and the quartz plate to eliminate birefringence due to the leads. The transmitted intensity versus wavelength was recorded for the polarizers in a crossed orientation. The 90-nm scan range (centered at 1525 nm) yielded multiple nulls corresponding to the condition that the retardance $\Delta nL/\lambda$ of the quartz plate was an integer. For the conditions described, those integers were near 77, depending on the order of null. Therefore, as long as our estimate of $\Delta nL/\lambda$ was better than 0.5 parts in 77 (0.65%), we would be able to determine the order number of a given null unambiguously. Then, forcing $\Delta nL/\lambda$ to be equal to that integer gives a more accurate estimate of Δn. As stated, published values of Δn differed by 0.18%. Since this uncertainty is significantly less than the required 0.65% (as are the 0.014% thickness uncertainty and the 0.0005% wavelength uncertainty), we can identify the order of each fringe. For example, using a literature value $\Delta n_{\mathrm{lit}}(\lambda)$, for a particular null λ_{null}, $\Delta n_{\mathrm{lit}}(\lambda_{\mathrm{null}})L/\lambda_{\mathrm{null}} = 77.009$. Our accuracy is good enough to say that the true order of this null is 77 (not 76 or 78). We then correct for the least accurate parameter $\Delta n_{\mathrm{lit}}(\lambda)$ so that $\Delta n_{\mathrm{corr}}(\lambda_{\mathrm{null}})L/\lambda_{\mathrm{null}} = 77$ exactly. Doing so over the 90-nm wavelength range, we have improved the accuracy of our Δn estimate by an order of magnitude

so that it is limited by the length uncertainty of 0.014%.

The PMD of the quartz plate is $\Delta nL/c$ (where c is the speed of light), and we found it to be equal to 0.4467 ps for a 89-nm scan centered at 1524.5 nm. The uncertainty on this number is due to the uncertainty of L (0.014%) and Δn ($\pm$0.014%). Adding in quadrature gives $\pm$0.02% or 0.09 fs. The birefringence of the fiber leads themselves was measured (in the absence of the quartz plate) to be approximately 1.2 fs. This is not an exact estimate of the error due to lead birefringence since as the leads are repositioned, the PMD of the leads add to or subtract from the PMD of the device. Moving the leads between measurements averages the effect of lead birefringence, but not completely. Some birefringence is likely to be in the graded-index lenses themselves, and their orientation does not change when the leads are moved. We therefore estimate the uncertainty on the PMD of the artifact to be the quadrature sum of the 0.09-fs uncertainty of the quartz plate and the 1.2 fs of the leads, giving an overall 1.2-fs uncertainty dominated by lead birefringence. We obtain an approximately 95% confidence interval by using a coverage factor of 2. Therefore we estimate the PMD of the pigtailed quartz plate to be 0.4467 $\pm$ 0.0024 ps at 1524.5 nm and 20.2 °C.

Our JME measurements of the quartz plate's PMD were carried out at a temperature of 23.3 $\pm$ 0.1 °C. We therefore modify our estimate of the PMD to this temperature. The thermal expansion of quartz, $\alpha = 13.6 \times 10^{-6}/°\mathrm{C}$ (Ref. 14) couples with the temperature dependence of the birefringence to give a temperature dependence to PMD. The temperature dependence of the retardance of quartz at 1525 nm is assumed equal to a value measured at 1535.59 nm,[15]

$$\gamma = (1/\Delta nL)\mathrm{d}(\Delta nL)/\mathrm{d}T = -1.232 \times 10^{-4}/°\mathrm{C}.$$

Using γ, we estimate the PMD of the quartz plate to be 0.4464 $\pm$ 0.0024 ps at 23.3 °C and 1524.5 nm.

References and Notes

1. P. A. Williams, "Mode-coupled artifact standard for polarization-mode dispersion: design, assembly, and implementation," Appl. Opt. **38,** 6498–6507 (1999).
2. B. L. Heffner, "Automated measurement of polarization mode dispersion using Jones matrix eigenanalysis," IEEE Photon. Technol. Lett. **4,** 1066–1069 (1992).
3. See "Polarization-mode dispersion measurement for single-mode optical fibers by Jones matrix eigenanalysis," *Fiber Optic Test Procedure (FOTP) 122* Telecommunications Industry Association, 2500 Wilson Blvd., Suite 300, Arlington, VA 22201 USA.
4. D. J. Ives, "Calibration of a polarisation state analyser for polarisation mode dispersion measurements," in *Technical Digest of the Fourth Optical Fibre Measurement Conference* (Teddington, UK, 1997), pp. 213–216. The exact form of the Stokes polarimeter in this reference is unclear, however, a detailed error analysis is carried out.
5. The terms type A and type B uncertainties refer to the ISO and the NIST convention and denote uncertainties that are (A) evaluated by statistical means and (B) evaluated by nonstatistical means. For details, see B. N. Taylor and C. E. Kuyatt, eds., "Guidelines for evaluating and expressing the uncertainty of NIST measurement results," National Institute of Standards and Technology, TechNote 1297 (National Institute of Standards and Technology, Boulder, Colo., 1994).
6. P. A. Williams, A. H. Rose, and C. M. Wang, "Rotating-polarizer polarimeter for accurate retardance measurement," Appl. Opt. **36,** 6466–6472 (1997).
7. P. D. Hale and G. W. Day, "Stability of birefringent linear retarders (waveplates)," Appl. Opt. **27,** 5146–5153 (1988).
8. K. B. Rochford, A. H. Rose, P. A. Williams, C. M. Wang, I. G. Clarke, P. D. Hale, and G. W. Day, "Design and performance of a stable linear retarder," Appl. Opt. **36,** 6458–6465 (1997).
9. E. Collette, ed., *Polarized Light: Fundamentals and Applications* (Marcel Dekker Inc., New York, 1993), p. 103.
10. J. H. Shields and J. W. Ellis, "Dispersion of birefringence of quartz in the near infrared," J. Opt. Soc. Am. **46,** 263–265 (1956).
11. W. L. Wolfe and G. J. Zissis, eds., *The Infrared Handbook* (Environmental Research Institute of Michigan, Ann Arbor, 1985), pp. 7–57.
12. B. L. Heffner, "Attosecond-resolution measurement of polarization mode dispersion in short sections of optical fiber," Opt. Lett. **18,** 2102–2104 (1993).
13. J. D. Jackson, *Classical Electrodynamics* (Wiley, New York, 1975), p. 302.
14. D. E. Gray, ed., *American Institute of Physics Handbook* (McGraw-Hill, New York, 1972), pp. 4–138.
15. A. H. Rose and S. M. Etzel, National Institute of Standards and Technology, Boulder, Colo., 80303 (personal communication).

Appendix D. Birefringence of Quartz

The wavelength dependent group birefringence $\Delta n_g(\lambda)$ of quartz is obtained from phase birefringence $\Delta n(\lambda)$ values found in the literature [8, 9]. When discussing birefringence, it is important to specify whether this is phase birefringence Δn or group birefringence Δn_g. The two are related as [15]

$$\Delta n_g = \Delta n - \lambda \frac{d\Delta n}{d\lambda}. \tag{D1}$$

Fig. D1 illustrates the differences in Δn and Δn_g for quartz over the wavelength range of interest. In practice, the phase birefringence is used in cases where the relative phases of light traveling in the two polarization eigenmodes is the parameter of interest. For example, the retardance δ of a single waveplate (thickness L) depends on the phase birefringence as $\delta=2\pi\Delta nL/\lambda$. Group birefringence is used when the parameter of interest is the difference in the velocity of energy flow between two polarization eigenstates. For example, the PMD of a single quartz plate comes from the difference in group velocity between the eigenstates, PMD = $\Delta n_g L/c$.

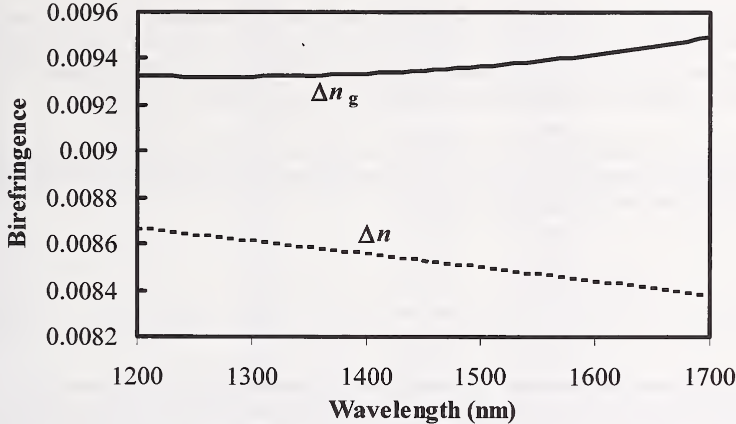

Figure D1. Spectral dependence of quartz phase (Δn) and group (Δn_g) birefringence.

We estimate the group birefringence of quartz by differentiating a fit to published $\Delta n(\lambda)$ data for crystal quartz [8, 9]. Only data in the wavelength range from 900 nm to 2000 nm were used for the fit. A total of 30 data points were fit with a third-order polynomial, yielding the coefficients:

$$a_0 = \frac{11910533.0}{1265000000.0},$$

$$a_1 = \frac{-150779.0}{189750000.0},$$

$$a_2 = \frac{31.0}{137500.0},$$

and

$$a_3 = \frac{-34.0}{474375.0}.$$

The coefficients are expressed in this fractional form to preserve their numerical precision. The phase birefringence is then given by

$$\Delta n(\lambda) = a_0 + a_1\lambda + a_2\lambda^2 + a_3\lambda^3, \qquad \text{(D2)}$$

where wavelength λ is in units of micrometers (μm). Substituting Eq. (D2) into Eq. (D1) gives the expression for group birefringence,

$$\Delta n_g(\lambda) = a_0 - a_2\lambda^2 - 2a_3\lambda^3, \qquad \text{(D3)}$$

(again, with λ in μm). The uncertainty in $\Delta n_g(\lambda)$ depends on the uncertainty of the polynomial coefficients, which comes from the covariance matrix of the fitted coefficients to $\Delta n(\lambda)$ [10] and includes the uncertainty of the literature $\Delta n(\lambda)$ values. Wavelength-dependent values of group birefringence of quartz and the associated uncertainty of Δn_g are given in Table D1.

For the purpose of extrapolating mean DGD measurements to other wavelengths, we require knowledge of the averaged value of Δn_g over the wavelength range of interest. The expression for this comes from the integral of Eq. (D3),

$$\langle \Delta n_g \rangle_{\lambda_1-\lambda_2} = \frac{\int_{\lambda_1}^{\lambda_2} \Delta n_g(\lambda)\, d\lambda}{\lambda_2 - \lambda_1} = a_0 - \frac{a_2}{3}(\lambda_1^{\ 2} + \lambda_1\lambda_2 + \lambda_1^{\ 2}) - \frac{a_3}{2}(\lambda_2 + \lambda_1)(\lambda_2^{\ 2} + \lambda_1^{\ 2}). \qquad \text{(D4)}$$

The uncertainty associated with this estimate of wavelength-averaged Δn_g depends on the uncertainty of the polynomial coefficients. Table D2 illustrates wavelength-averaged group birefringence and the associated uncertainty $U(\langle \Delta n_g \rangle)$ for quartz over a set of wavelength ranges.

Table D1. Estimated group birefringence $\Delta n_g(\lambda)$ and associated uncertainty $U(\Delta n_g(\lambda))$ for quartz at the stated wavelength (not a wavelength-averaged value). This table can be used to estimate $\Delta n_g(\lambda)$ and $U(\Delta n_g(\lambda))$values for any wavelength from 1200 to 1700 nm with a 1 nm increment. Values for wavelengths omitted from the table are equal to the values at the previous printed wavelength.

Wavelength (nm)	$\Delta n_g(\lambda)$	$U(\Delta n_g(\lambda))$
1200	0.00934	0.000018
1244	0.00934	0.000019
1267	0.00935	0.000019
1268	0.00935	0.000020
1287	0.00935	0.000021
1305	0.00935	0.000022
1323	0.00935	0.000023
1337	0.00936	0.000023
1342	0.00936	0.000024
1362	0.00936	0.000025
1387	0.00936	0.000026
1391	0.00937	0.000026
1422	0.00937	0.000027
1436	0.00938	0.000027
1476	0.00939	0.000027
1510	0.00939	0.000026
1511	0.00940	0.000026
1543	0.00941	0.000026
1547	0.00941	0.000025
1572	0.00942	0.000025
1575	0.00942	0.000024
1599	0.00943	0.000024
1602	0.00943	0.000023
1625	0.00944	0.000023
1649	0.00945	0.000023
1672	0.00946	0.000023
1683	0.00946	0.000024
1694	0.00947	0.000024
1698	0.00947	0.000025
1700	0.00947	0.000025

Table D2. Estimated wavelength-averaged group birefringence $\langle \Delta n_g \rangle_{\lambda_1-\lambda_2}$ and associated uncertainty $U(\langle \Delta n_g \rangle_{\lambda_1-\lambda_2})$ for quartz, averaged over the range from λ_1 to λ_2

λ_1 (nm)	λ_2 (nm)	$\langle \Delta n_g \rangle_{\lambda_1-\lambda_2}$	$U(\langle \Delta n_g \rangle_{\lambda_1-\lambda_2})$
1200	1250	0.009341	0.000018
1200	1300	0.009343	0.000019
1200	1350	0.009347	0.000020
1200	1400	0.009350	0.000020
1200	1450	0.009355	0.000021
1200	1500	0.009360	0.000022
1200	1550	0.009366	0.000022
1200	1600	0.009372	0.000022
1200	1650	0.009379	0.000022
1250	1300	0.009346	0.000020
1250	1350	0.009350	0.000021
1250	1400	0.009354	0.000022
1250	1450	0.009358	0.000023
1250	1500	0.009364	0.000024
1250	1550	0.009370	0.000024
1250	1600	0.009376	0.000023
1250	1650	0.009384	0.000023
1300	1350	0.009353	0.000023
1300	1400	0.009358	0.000024
1300	1450	0.009363	0.000024
1300	1500	0.009368	0.000025
1300	1550	0.009374	0.000025
1300	1600	0.009381	0.000024
1300	1650	0.009389	0.000024
1350	1400	0.009362	0.000025
1350	1450	0.009367	0.000026
1350	1500	0.009373	0.000026
1350	1550	0.009380	0.000026
1350	1600	0.009387	0.000025
1350	1650	0.009395	0.000024
1400	1450	0.009373	0.000027
1400	1500	0.009379	0.000027
1400	1550	0.009386	0.000026
1400	1600	0.009393	0.000026
1400	1650	0.009402	0.000024
1450	1500	0.009385	0.000027
1450	1550	0.009392	0.000026
1450	1600	0.009400	0.000025
1450	1650	0.009409	0.000024
1500	1550	0.009400	0.000026
1500	1600	0.009408	0.000025
1500	1650	0.009417	0.000024
1550	1600	0.009416	0.000024
1550	1650	0.009426	0.000023
1600	1650	0.009435	0.000023
1480	1570	0.009400	0.000026